

Symmetry Breaking in Grand Unified and Flavour Theories

A Systematic Study of $SO(10)$ Subalgebras and A_4 Emergence from $SU(3)$

Annick van Akker



Supervised by: Prof. Dr. Daniël Boer
Faculty of science and engineering
Rijksuniversiteit Groningen
16-12-2025

Abstract

Symmetry breaking in Grand Unified Theories (GUTs) is governed by the structure of subalgebras of the Lie algebra of the unified gauge group and the Vacuum Expectation Values (VEVs) that realise specific breaking chains. This thesis develops a systematic framework for understanding such breaking patterns, classifying the regular and special subalgebras of the $SO(10)$ Lie algebra and determining the corresponding VEV textures. Next, we consider discrete symmetries emerging from the breaking of global continuous symmetry groups, focusing on $A_4 \subset SU(3)$, motivated by the role of A_4 in explaining neutrino mixing structures. We demonstrate that specific VEVs in $SU(3)$ representations break the symmetry to A_4 . We discover that the order of the application of these VEVs matters. The methods and frameworks obtained here provide practical tools for constructing and justifying symmetry-breaking patterns in Beyond-the-Standard-Model physics.

Contents

1	Introduction	3
2	Lie groups and their structures	6
2.1	Lie Groups	6
2.1.1	Representations and Irreducible Representations	7
2.1.2	Schur's lemma	7
2.1.3	Roots, Weights and the Cartan Subalgebra	7
2.2	Subalgebras	11
2.2.1	Projection Matrices	11
2.2.2	Regular Subalgebras	12
2.2.3	Special Subalgebras	12
2.3	$SU(3)$	14
2.3.1	Subalgebras of $SU(3)$	16
2.4	$SU(5)$	20
2.5	$SO(10)$	21
3	VEVs of Continuous Groups	24
3.1	$SU(2) \times U(1)$	24
3.1.1	Higgs doublet	24
3.1.2	Different VEVs	27
3.2	$SU(3)$	29
3.3	$SO(10)$	32
3.3.1	Methodology for finding VEV textures	34
3.3.2	Connection to other research	38
4	Residual discrete symmetries from $SU(3)$	42
4.1	A_4 leading to Tri-bimaximal Mixing	43
4.2	$SU(3) \rightarrow A_4$	43
4.3	Different order of VEVs	47
5	Conclusion	51
5.1	Main Results	51
5.1.1	$SO(10)$ Breaking Patterns	51
5.1.2	$SU(3) \rightarrow A_4$ breaking	52
5.1.3	Order dependence	52

5.2	Future Research	52
5.3	Broader Implications	53
5.3.1	Phenomenological implications of VEV ordering	53
5.3.2	Implications for Model Building	53
	Acknowledgements	54
6	Appendix	58
6.1	Generators of finite groups of $SU(3)$	58
6.2	Generators of finite groups of $SO(3)$	59

Chapter 1

Introduction

Symmetry principles and group theory lie at the heart of modern theoretical physics, providing a unifying language for understanding the fundamental structures of nature. Beyond the Standard Model (BSM) theories often rely on large symmetry groups whose spontaneous breaking gives rise to the observed structure of the Standard Model (SM). One of the most studied frameworks in this context is Grand Unified Theories (GUTs), which aim to unify the strong, weak and electromagnetic forces into a single gauge group. The GUTs are typically based on large, simple Lie groups, such as $SU(5)$ and $SO(10)$, which contain the SM gauge group, $SU(3)_c \times SU(2)_L \times U(1)_Y$, as a subgroup.

Despite decades of progress, the full landscape of possible symmetry-breaking patterns within large gauge groups remains only partially explored. This has important physical consequences: different breaking chains predict different proton decay rates, gauge coupling unification scales, and intermediate symmetries. The literature predominantly focuses on specific chains to the Standard Model, such as $SO(10) \rightarrow SU(5) \rightarrow SU(3)_c \times SU(2)_L \times U(1)_Y$ and $SO(10) \rightarrow SU(4) \times SU(2) \times SU(2) \rightarrow \text{SM}$. This emphasis is well-motivated as $SO(10)$ is able to provide a minimal extension of the Standard Model, where all fifteen fermions plus a right-handed neutrino fit into one single 16-dimensional spinor representation. However, this perfect fit does not uniquely determine which symmetry-breaking path $SO(10)$ actually follows. As we illustrate in section 3.3.2, different scalar field representations lead to different breaking patterns. This work was done by Magnus Petz in [32], based on the work by Held et al. in [23]. Here it is seen that even after choosing a specific scalar representation, the resulting breaking chain depends on the values of parameters in the scalar potential. The structure of the vacuum is determined by minimising this potential, but most commonly studied chains may not even correspond to the global minimum as this has never been fully researched. Different chains correspond to different vacuum energies and we cannot simply assume the commonly studied patterns correspond to the global minimum, without proper verification.

Beyond gauge unification, GUT groups do not address another puzzle: the origin of flavour structure. Fermion masses span from $\sim 10^{-2}$ eV for neutrinos to ~ 173 GeV for the top quark—thirteen orders of magnitude [15]. Moreover, fermion mixing shows a striking contrast between sectors. In the lepton sector, neutrino oscillations reveal two mixing an-

gles near maximal, corresponding to angles near 45° and so to an almost equal mixture of flavour states, while the third angle remains small. This pattern is drastically different from the hierarchical quark mixing angles, where all angles are small and very hierarchical. This contrast demands different underlying structures.

A global $SU(3)$ flavour symmetry acting on three fermion generations provides a framework to explain these hierarchies. At high energies, $SU(3)$ treats families as a triplet; breaking at lower scales generates hierarchical mass textures. However, exact continuous flavour symmetry cannot survive to low energies, as this would predict equal masses for all generations. Instead, a discrete residual symmetry must emerge, with different breaking patterns in quark and lepton sectors explaining their contrasting mixing.

This thesis systematically maps out this landscape, developing tools for identifying all possible subalgebras and symmetry-breaking chains within GUT groups, and understanding how discrete subgroups emerge. This creates a framework for future researchers to clearly show which textures they need and why—explanation often missing in current work.

This work is organised around three key objectives:

1. **Subalgebra Classification:** Identify all maximal subalgebras of a given Lie group using Dynkin diagrams and root systems. We focus on $SO(10)$ as a representative GUT and on $SU(3)$ for discrete subgroup formation.
2. **VEV Texture Analysis:** For each breaking pattern, determine the minimal VEV configurations achieving the desired reduction. We identify the minimal scalar representation containing a singlet under the desired subgroup and construct explicit VEV configurations.
3. **Discrete Symmetry Emergence:** Investigate conditions under which discrete subgroups, specifically $A_4 \subset SU(3)$, arise from continuous symmetry breaking. Unlike continuous cases, discrete symmetries require verifying that finite group elements leave the VEV invariant.

Parts of the Mathematica code developed in this thesis was assisted by the AI language models, Claude [4] and ChatGPT [30]. All mathematical analysis, interpretations and validations were of course performed independently.

We focus specifically on A_4 , the alternating group on four elements, because it is the smallest finite group with a three-dimensional irreducible representation, making it minimal for treating three generations as a triplet. The phenomenological motivation comes from neutrino physics. Experimental results are approximately consistent with tri-bimaximal mixing (TBM): $\theta_{12} \approx 35^\circ$, $\theta_{23} = 45^\circ$, and $\theta_{13} = 0^\circ$ [15]. While modern experiments, particularly Daya Bay (2022) have precisely measured $\sin^2(2\theta_{13}) = 0.0851 \pm 0.0024$ [3]. This corresponds to $\theta_{13} \approx 8.5^\circ$, ruling out exact tri-bimaximal mixing. However, the observed pattern remains close to this form and A_4 models with appropriately broken symmetry remain viable [2, 15, 33].

Understanding how A_4 emerges from $SU(3)$ breaking connects flavour physics to the spontaneous symmetry breaking mechanism governing electroweak breaking and grand unification.

To summarise, this research provides a framework enabling systematic exploration of which breaking patterns are possible before determining which are realized. For $SO(10)$, we catalogue all possible breaking chains so dynamical studies can determine which route minimises the potential. For $SU(3)$ flavour symmetry, we demonstrate how A_4 emerges from continuous breaking and reveal that the order of VEV application matters, which is an unexpected result.

Chapter 2

Lie groups and their structures

Symmetry is crucial in modern theoretical physics and forms the foundation of fundamental interactions. Group theory provides a mathematical framework to describe these symmetries. In particular, Lie groups and their corresponding Lie algebras are essential tools in Quantum Field Theory and particle physics. These groups form the backbone of gauge theories and Grand Unified Theories (GUTs). The following section will give an overview of the necessary mathematical structures, starting with a brief introduction to group theory. We then move on to Lie groups and Lie algebras, which describe the continuous symmetries, followed by an introduction to their representations, weight and root systems and subalgebras, which are essential for understanding the classification and breaking of symmetries in high-energy physics.

2.1 Lie Groups

To understand the content of this thesis, a basis of group theory is necessary. Here we will briefly cover the basics as discussed by [11], [34] and [24].

A group G is a mathematical structure consisting of a set of elements together with a group multiplication \circ that satisfies the following axioms for all elements $g_i \in G$:

Closure: $g_i \circ g_j \in G$

Associativity: $(g_i \circ g_j) \circ g_k = g_i \circ (g_j \circ g_k)$

Identity: There exists $e \in G$ such that $e \circ g_i = g_i \circ e = g_i$

Inverse: For each $g_i \in G$, there exists $g_i^{-1} \in G$ such that $g_i \circ g_i^{-1} = g_i^{-1} \circ g_i = e$

The set of elements of the group is either discrete or continuous. If they are the latter, we are talking about Lie groups. Formally, a Lie group is a differentiable manifold which also acts as a group, with the group multiplication $\circ : G \times G$, and the maps that send $g \in G$ to its inverse $g^{-1} \in G$, are differentiable maps. Some important examples we will be using are $SO(N)$ and $SU(N)$. The $SO(N)$ groups are the special orthogonal groups that consist of orthogonal matrices with a determinant equal to 1. The $SU(N)$ groups are the

special unitary group that consists of unitary matrices with a determinant equal to 1. In this research project we will primarily focus on the groups $SO(10)$, $SU(3)$ and $SU(5)$.

Lie groups can be analysed locally by looking at their respective Lie algebras. A Lie algebra \mathfrak{g} is a vector space equipped with a binary operation $[\cdot, \cdot] : \mathfrak{g} \times \mathfrak{g} \rightarrow \mathfrak{g}$ called the Lie product satisfying:

1. **Bilinearity:** The bracket is linear in both arguments
2. **Antisymmetry:** $[X, Y] = -[Y, X]$ for all $X, Y \in \mathfrak{g}$
3. **Jacobi identity:** $[X, [Y, Z]] + [Y, [Z, X]] + [Z, [X, Y]] = 0$ for all $X, Y, Z \in \mathfrak{g}$

In this thesis, we focus on a specific class of Lie groups that are relevant for particle physics, namely compact and simple Lie groups. These groups underlie the structure of gauge theories and GUTs and their mathematical properties allow for well-behaved representation theory and symmetry breaking patterns. A Lie group is called compact if the parameters range over a closed and bounded set, i.e. compact set. Examples of compact Lie groups are $SU(N)$ and $SO(N)$. A Lie group is simple if it has no proper invariant Lie subgroup. A subgroup $H \subseteq G$ is invariant if for all elements $h \in H$ and $g \in G$: $ghg^{-1} \in H$.

2.1.1 Representations and Irreducible Representations

Representations of a group offer a way of describing the elements of the group as matrices, acting on a space of vectors, such that group multiplication corresponds to matrix multiplication. Formally, we describe representations of a group G as a homomorphism $D : G \rightarrow GL(V)$, where $GL(V)$ is the group of invertible linear transformations on a vector space V . A representation is said to be irreducible, or irrep for short, if there is no non-trivial invariant subspace under all group actions. This means it cannot be decomposed into smaller representations. Irreps are the building blocks of all other representations and any finite-dimensional representation of a compact Lie group can be decomposed into irreducible ones.

2.1.2 Schur's lemma

An important part of representation theory is Schur's lemma, which states the following for compact Lie groups:

A unitary rep $D : G \rightarrow GL(d, \mathbf{k})$ of a Lie group G is an irrep iff the only matrices commuting with $D(g), \forall g \in G$, are (complex) scalar multiples of the unit matrix.[11]

This lemma tells us that the only operators, which are matrices for this thesis, that commute with all group actions in an irrep are multiples of the identity.

2.1.3 Roots, Weights and the Cartan Subalgebra

The structure of Lie algebras can be studied via their characteristic root systems, which determine the structure and the irreps of the Lie algebras. To understand these, we will review all relevant concepts, including roots and weights.

A fundamental structure of Lie algebras is the Cartan subalgebra. This is a maximal diagonalisable Abelian subalgebra that is composed of the maximal set of commuting generators $[H_i, H_j] = 0, i, j = 1, \dots, r$, where the total number of commuting generators r is equal to the rank of the algebra. This means that the dimension of the Cartan subalgebra is equal to the rank of the algebra. The remaining generators of the Lie algebra satisfy eigenvalue equations of the form: $[H_i, E_\alpha] = \alpha_i E_\alpha, i = 1, \dots, r$. For each operator E_α , there are r eigenvalues $\alpha_1, \dots, \alpha_r$. The solution to the eigenvalue equation is called the root vector $(\alpha_1, \dots, \alpha_r)$, or root for short. The set of roots forms a root system, which determines the structure of the algebra. Roots have some important properties. First, if α is a root then $-\alpha$ is also a root. Secondly, the roots are non-degenerate which means that they all correspond to a unique generator. Lastly, the roots can be used to classify the Lie algebra using Dynkin diagrams.

The Dynkin diagram is a graphical tool to represent the roots of a Lie algebra and is built up of simple roots. Simple roots form a basis for all roots, where the simple roots are not linearly dependent on other roots. We often describe the simple roots as either negative or positive, depending on the convention we use. For this thesis we define the simple roots as positive roots, that again cannot be decomposed into sums of other positive roots. These simple roots are represented as circles and the lines connecting the roots represent the angles between the roots. In the cases where the roots have different lengths, the open circle \circ represents the longer simple roots and the filled circle \bullet represents the shorter simple root. To see how the angle between the simple roots determines the Dynkin diagram, see table 2.1.

θ_{12}	$ \alpha_1 / \alpha_2 $	Dynkin
90°		$\circ \circ$
120°	1	$\circ - \circ$
135°	$\sqrt{2}$	$\circ - \bullet$
150°	$\sqrt{3}$	$\circ - \bullet$

Table 2.1: Dynkin diagrams corresponding to the relative angles and lengths of two simple roots α_1 and α_2 , assuming $|\alpha_1| \geq |\alpha_2|$. Adapted from [34].

Using the table 2.1, we can represent all Lie algebras by a Dynkin diagram. It is important to emphasise that the classification is given for complex Lie algebras. Each complex algebra admits multiple real forms. This means that a single Dynkin diagram corresponds not to one real Lie algebra but rather to a finite set of real Lie algebras obtained from the complexified algebra.

The classification of complex, simple Lie algebras, or equivalently of connected Dynkin diagrams, is divided into four infinite families, known as the classical series, A_n, B_n, C_n and D_n , and five exceptional cases, denoted as G_2, F_4, E_6, E_7 and E_8 .

While roots describe the structure of the Lie algebra itself, the weights describe the algebra in representation space. Consider a representation D of a Lie algebra, with H_j denoting

Category	Lie group	Dynkin diagram
A_n	$\widetilde{su}(n+1)$, for $n \geq 1$	
B_n	$\widetilde{so}(2n+1)$, for $n \geq 1$	
C_n	$\widetilde{sp}(2n)$, for $n \geq 1$	
D_n	$\widetilde{so}(2n)$, for $n \geq 3$	
G_2		
F_4		
E_6		
E_7		
E_8		

Table 2.2: The Lie algebras and their corresponding Dynkin diagrams

the representation of the Cartan subalgebra generators. A vector $|m\rangle$ in the representation space is a weight vector if it is a simultaneous eigenvector of all H_j :

$$H_j|m\rangle = m_j|m\rangle, \quad (2.1)$$

where the weight vector $m = (m_1, \dots, m_r)$ is called the weight that is associated with $|m\rangle$ and r is the rank of the algebra.

The set of all these eigenvectors $\{|m\rangle\}$ then forms a complete basis of the representation, since the remaining non-diagonal generators E_α act as ladder operators. These ladder operators connect the weight states according to: $E_\alpha|m\rangle \propto |m + \alpha\rangle$. Each pair of the ladder operators, $(E_{+\alpha}, E_{-\alpha})$, together with the corresponding Cartan element forms an $\mathfrak{su}(2)$ subalgebra. The representation theory of these $\mathfrak{su}(2)$ subalgebras ensures that, starting from the highest-weight state, repeated action of the ladder operator generates all other states in the irreducible representation.

Since every state can be obtained from the highest-weight state by applying these lowering operators, and the lowering operators always produce new weights, the full irreducible representation is spanned by its weight vectors. This means that the weight vectors form the basis of any irreducible representation.

The procedure to find weights is very similar to that of roots. The difference is that roots can be seen as weights of the adjoint representation. A weight m can be written in terms of simple roots as $m = \sum \mu_i \alpha_i$, where μ_i are real and rational coefficients. If the first non-vanishing coefficient μ_i is positive, the weight is positive. The highest weight M is such that $M > m$ for all other weights of the representation. Irreps are uniquely specified by their

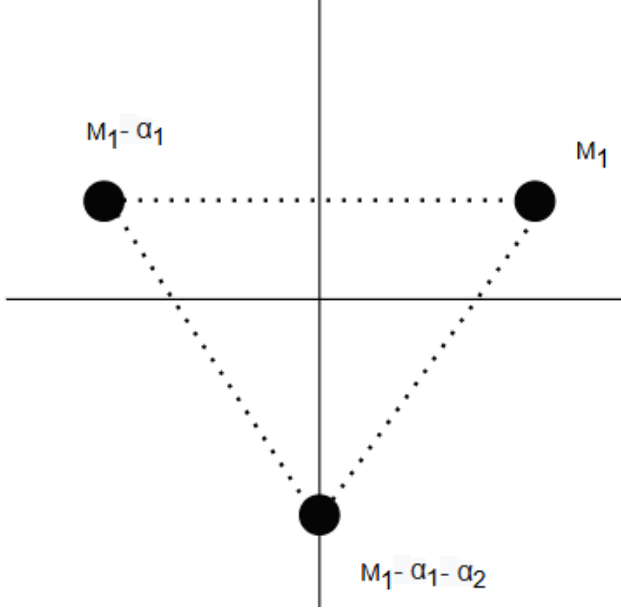


Figure 2.1: Weight diagram of the fundamental representation of $\mathfrak{su}(3)$, with the highest weight M_1 .

highest weight. Fundamental weights, M_i , satisfy

$$\frac{2M_i \cdot \alpha_i}{\alpha_j \cdot \alpha_j} = \delta_{ij}, \quad (2.2)$$

for all simple roots α_j . The fundamental weights can be seen as the natural basis vectors for the weight space in the same way as simple roots are the basis vectors for the root system. The fundamental weights can be used to find the highest weight, following: $M = \sum_{i=1}^r n_i M_i$. Here, n_i are non-negative integers called Dynkin labels. By using these Dynkin labels, the values for roots and weights all become integers, meaning that calculations are more simplified. The Dynkin label n_j of a weight vector α_j is determined with the following formula:

$$n_j = \frac{2M \cdot \alpha_j}{\alpha_j \cdot \alpha_j} \quad (2.3)$$

To make this more concrete, consider $SU(3)$, whose root system lives in a two dimensional plane. The two fundamental weights M_1 and M_2 are dual to the two simple roots α_1 and α_2 , and every weight can be written as $M = n_1 M_1 + n_2 M_2$. As an example, the defining, or fundamental, representation of $SU(3)$ has Dynkin labels $(1, 0)$. The anti-fundamental on the other hand has the Dynkin labels $(0, 1)$. The weight diagram of these representations can then be drawn explicitly. The weight diagram for the fundamental representation forms an equilateral triangle in the plane, with the weights at positions M_1 , $M_1 - \alpha_1$ and $M_1 - \alpha_1 - \alpha_2$. This is visualised in figure 2.1. Similarly, other representations can be visualised as sets of points in the plane, labelled by their weights.

2.2 Subalgebras

Subalgebras play an important role in studying the symmetry-breaking mechanisms and model-building in GUTs. By identifying the subalgebras of a given Lie algebra, we can understand how a larger symmetry group can be decomposed into smaller parts. Mathematically, a proper subalgebra L' of the Lie algebra $L' \subset L$ is defined as the set of elements in L , with the same Lie product as L , and if for each pair of elements in L' , $a, b \in L'$, their Lie product is also in the subalgebra [11]:

$$[a, b] \in L' \quad (2.4)$$

We are dealing with an invariant subalgebra of the Lie algebra L , it is a subalgebra and if for all $a' \in L'$ and all $b \in L$, $[a', b] \in L'$.

For this research, we are interested in two types of subalgebras, the regular and special subalgebras. In the following paragraphs, we will discuss these, but first we will discuss a handy tool for decomposing irreps of an algebra into irreps of a subalgebra, the projection matrix.

2.2.1 Projection Matrices

To understand how different subalgebras embed into different algebras at the level of representations, it is useful to work with projection matrices. The projection matrix relates the fundamental weights of the subalgebra to those of the parent algebra. The information covered here is based on [18], [34] and [38].

For regular embeddings, the projection matrix can often be read off from the Dynkin diagram by considering which simple roots are kept and how they relate to the roots of the subalgebra. In the case of regular embeddings, this procedure is especially straightforward, as the subalgebra corresponds to a subset of nodes in the Dynkin diagram. This means that we pick certain simple roots from the original root system and these then correspond directly to the subalgebra's Dynkin diagram nodes. For special embeddings, the projection can be determined using these root correspondences, but they have an extra characteristic: an irreducible representation of a larger algebra remains irreducible under restriction to the subalgebra.

There is a projection matrix for any subalgebra, whether they are special or regular. To construct the projection matrix, a simple matrix calculation is needed. Suppose we want to find the projection matrix that takes the roots and weights of G , with rank r_G onto the roots and weights of H , with rank r_H . We can then project any weight of a representation of G onto the corresponding weight of H , by a matrix acting as

$$P(G \supset H) \cdot \vec{a} = \vec{b} \quad (2.5)$$

The projection matrix acts on weights, but also the roots of G that are viewed as weights of the adjoint representation. After projection, they become weights of representations of H . In equation 2.5, $P(G \supset H)$ is the $r_H \times r_G$ projection matrix, $\vec{a} = (a_1, \dots, a_{r_G})^T$ a weight of G and $\vec{b} = (b_1, \dots, b_{r_H})^T$ the projected weight in H . In the specific cases covered in this thesis, the projection matrices will be explicitly calculated, however, programmes such as LieArt also offer a way to determine the projection matrix without calculations by hand. More information on this can be found in the LieArt literature [18].

2.2.2 Regular Subalgebras

Regular subalgebras, or R-subalgebras as they are also called in literature, are easily obtained by looking at the extended Dynkin diagram. This diagram consists not only of simple roots, which are all linearly independent, but there is an extra root added, the so-called lowest root. This root cannot be chosen at random, but has to be the negative of the highest root. This is because the difference between the roots in the diagram cannot be another root. The negative of the highest root makes sure that this, and the other criteria of the Dynkin diagram, are upheld, except for the linear independence [34]. Most extended Dynkin diagrams are listed in [34]. After adding this lowest root, often labelled with an x or a zero, we can obtain the regular subalgebras by removing one of the roots, or nodes, from the diagram. By removing a root like this from the diagram, the angle between the remaining roots can also change. This needs to be reflected into the Dynkin diagram by adding or removing a line between the two relevant roots, per the rules in table 2.1.

2.2.3 Special Subalgebras

A subalgebra $\mathfrak{h} \subset \mathfrak{g}$ is special if there exists at least one nontrivial irreducible representation of \mathfrak{g} that remains irreducible when restricted to \mathfrak{h} . This definition follows the classification introduced by Dynkin and later summarised by Slansky [16], [34]. To obtain the special subalgebras, we need more knowledge of the representations of the Lie algebra. A first method is to look into the exact generators in a given representation. Another method is to use the structure of the Dynkin diagram, and manipulate it to reveal the special subalgebra.

Before identifying candidate subalgebras, two facts must hold:

1. The dimension of the subalgebra must be equal to or smaller than the parent algebra
2. The rank of the subalgebra must be equal to or smaller than that of the parent algebra

While these conditions are trivial, they are necessary, as they restrict the algebra types possible.

When we want to know the special subalgebra of a certain group, there are a few steps to follow.

1. Use the Dynkin diagram of the Lie algebra to identify possible subalgebras

2. Once a candidate subalgebra is identified, its embedding can be verified using projection matrices, which map a weight of the parent algebra onto the weight of the subalgebra. This allows one to check directly whether the subalgebra acts irreducibly on the relevant representations.
3. Finally, the Weyl dimension formula can be used to confirm that the dimensions of the restricted irreps match the original irreps. This provides a final check of the special embedding.

To explain the steps of this guide, let us go through them in order. The first step is to use the Dynkin diagram of the Lie algebra. The Dynkin diagram of the parent algebra can be manipulated in several ways, each giving rise to a different subalgebra. There are the following algebraic operations to manipulate the Dynkin diagram:

- Node deletion: Removing one or more nodes of the Dynkin diagram. While removing one node of the extended diagram leads to a regular subalgebra, removing one or more nodes from the original Dynkin diagram itself could lead to different structures.
- Diagram folding: If the Dynkin diagram has a symmetry, an outer automorphism, nodes related by this symmetry can be identified. When a diagram is folded, these nodes collapse into a single node whose label respects the combined length and multiplicity of the original roots. As an example, folding D_4 along its triality symmetry produces the exceptional algebra G_2 . This is how Dynkin diagram folding produced special embeddings [40].
- Combining the two operations above.

By manipulating the Dynkin diagram using these algebraic operations, special subalgebras can be found. In this thesis, we verify the candidate embeddings using projection matrices, which maps the weight vectors of \mathfrak{g} to weight vectors of \mathfrak{h} . This makes it possible to explicitly verify irreducibility and branching rules for specific representations, which is essential when confirming that a subalgebra is indeed special.

Now, to finally verify whether this subalgebra is special, the dimension of the irreps must be equal. To check dimensionality of the representations, we can use the Weyl dimension formula [18]:

$$\dim(\Lambda) = \prod_{\alpha \in \Delta^+} \frac{(\alpha, \Lambda + \delta)}{(\alpha, \delta)} \quad (2.6)$$

Here, the dimension of the irrep is given in terms of its highest weight Λ , the positive roots $\alpha \in \Delta^+$ and the Weyl vector δ , defined as:

$$\delta = \frac{1}{2} \sum_{\alpha \in \Delta^+} \alpha. \quad (2.7)$$

This is the half-sum all positive roots. When expressed as coefficients of the fundamental weights, the Weyl vector is of the simple form: $\delta = (1, 1, \dots, 1)$, where the rank of the algebra

determines the number of 1's.

To calculate the dimensions of the irreps in this paper, the function `WeylDimensionFormula[Algebra]` in LieArt is used, which gives the explicit Weyl dimension formula for the chosen algebra, as a function of the Dynkin labels $(\lambda_1, \dots, \lambda_r)$ of the highest weight [17].

In the next chapter we will look at the specific cases $SU(5)$ and $SO(10)$ but first we will closely investigate the case of $SU(3)$.

2.3 $SU(3)$

The special unitary group $SU(3)$ is a Lie group that consists of 3×3 unitary matrices with a determinant equal to one. It is a compact, simple Lie group of rank 2 and dimension 8. As with all compact Lie group, the generators of $SU(3)$ satisfy the commutation relations:

$$[T_a, T_b] = i f_{abc} T_c, \quad (2.8)$$

where f_{abc} are the structure constants of the Lie algebra $\mathfrak{su}(3)$.

The Lie algebra $\mathfrak{su}(3)$ is spanned by eight generators, often represented by the Gell-Mann matrices, so $t_a = \frac{\lambda_a}{2}$. These are all hermitian and traceless.

$$\begin{aligned} \lambda_1 &= \begin{pmatrix} 0 & 1 & 0 \\ 1 & 0 & 0 \\ 0 & 0 & 0 \end{pmatrix}, & \lambda_2 &= \begin{pmatrix} 0 & -i & 0 \\ i & 0 & 0 \\ 0 & 0 & 0 \end{pmatrix}, & \lambda_3 &= \begin{pmatrix} 1 & 0 & 0 \\ 0 & -1 & 0 \\ 0 & 0 & 0 \end{pmatrix}, \\ \lambda_4 &= \begin{pmatrix} 0 & 0 & 1 \\ 0 & 0 & 0 \\ 1 & 0 & 0 \end{pmatrix}, & \lambda_5 &= \begin{pmatrix} 0 & 0 & -i \\ 0 & 0 & 0 \\ i & 0 & 0 \end{pmatrix}, & \lambda_6 &= \begin{pmatrix} 0 & 0 & 0 \\ 0 & 0 & 1 \\ 0 & 1 & 0 \end{pmatrix}, \\ \lambda_7 &= \begin{pmatrix} 0 & 0 & 0 \\ 0 & 0 & -i \\ 0 & i & 0 \end{pmatrix}, & \lambda_8 &= \frac{1}{\sqrt{3}} \begin{pmatrix} 1 & 0 & 0 \\ 0 & 1 & 0 \\ 0 & 0 & -2 \end{pmatrix} \end{aligned}$$

To form the Cartan subalgebra, we need commuting generators. Typically, λ_3 and λ_8 are chosen as they are already diagonal. The Cartan generators are then often defined as:

$$C_1 = \frac{\lambda_3}{2}, C_2 = \frac{\lambda_8}{2} \quad (2.9)$$

The weights of $\mathfrak{su}(3)$ can then easily be determined to be the components of the Cartan generators on the diagonal, since the Cartan generators themselves are diagonal. This then gives the weights the following form: $\mu_i = (C_{1ii}, C_{2ii})$. This then gives us the following three weights of the $\mathfrak{su}(3)$ Lie algebra in the fundamental rep **3**,

$$\mu_1 = \left(\frac{1}{2}, \frac{\sqrt{3}}{6} \right), \quad \mu_2 = \left(-\frac{1}{2}, \frac{\sqrt{3}}{6} \right), \quad \mu_3 = \left(0, -\frac{\sqrt{3}}{3} \right) \quad (2.10)$$

In the $SU(3)$ fundamental representation, these weights then give the following roots, which are the difference between two of the weights.

$$\pm\alpha_1 = \pm(1, 0), \pm\alpha_2 = \pm\left(-\frac{1}{2}, \frac{\sqrt{3}}{2}\right), \pm\alpha_3 = \pm\left(\frac{1}{2}, \frac{\sqrt{3}}{2}\right) \quad (2.11)$$

The fact that the difference between the weights corresponds to a root is not a general rule, but is the case here since the fundamental representation is fully connected by the algebra's raising and lowering operators. These operators are the six leftover generators after forming the Cartan subalgebra with two of the eight generators that span $SU(3)$. These raising and lowering operators E_α then are those with one non-zero off-diagonal component and can be defined using the Gell-Mann matrices as:

$$E_{\pm\alpha_1} = \frac{1}{2}(\lambda_1 \pm i\lambda_2) \quad E_{\pm\alpha_2} = \frac{1}{2}(\lambda_6 \pm i\lambda_7) \quad E_{\pm\alpha_3} = \frac{1}{2}(\lambda_4 \pm i\lambda_5) \quad (2.12)$$

The roots can thus be found using the difference in weights in this specific case and generally by using the raising and lowering operators.

We can now arrange these roots in a diagram, creating the root diagram of $SU(3)$, which consists of six nonzero roots arranged in a hexagonal pattern as can be seen in figure 2.2.

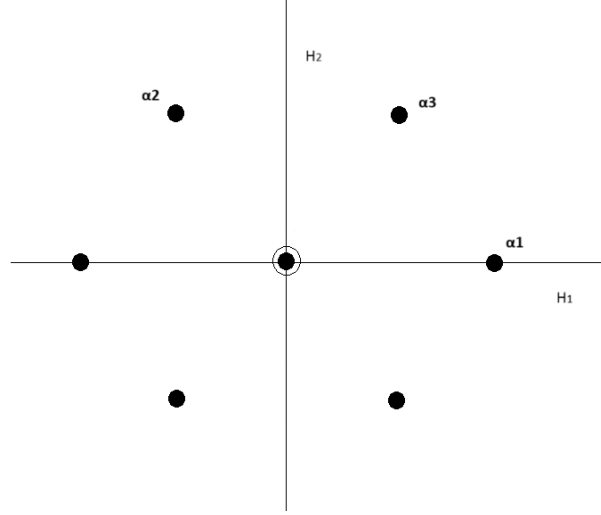


Figure 2.2: Root diagram of $SU(3)$. The two circles at the centre of the diagram corresponds to the two Cartan generators. These are two zero roots.

Now, to draw the Dynkin diagram, we need to find the simple roots, so the roots that are positive and not linearly dependent on other roots. The set of simple roots is however not uniquely determined as it depends on the choice of positive root system. For this thesis, we take all positive roots to be the ones that have a positive x-coordinate. This means that α_2 and α_3 are simple roots, since they are positive and linearly independent, while $\alpha_1 = \alpha_2 + \alpha_3$, which means that this is not a simple root. Since the rank of $SU(3)$ is 2, it is correct that

there are 2 simple roots, as the rank is equal to the amount of simple roots. This then means that the Dynkin diagram of $SU(3)$ consists of two nodes connected by a single line:

○—○

Each node corresponds to a simple root, and the connection between them indicates the angle between the simple roots. There is only a single line between the nodes, as there is an angle of 120° between the simple roots, as can be seen from the root diagram.

Now that we have an understanding of the structure of the algebra $\mathfrak{su}(3)$, we can move on to its subalgebras.

2.3.1 Subalgebras of $SU(3)$

As has been explained before, the regular subalgebra of an algebra can simply be determined by removing a node from the Dynkin diagram. As determined before, the Dynkin diagram of $SU(3)$ is the following:

○—○

Now, by removing a node from the Dynkin diagram, does not matter which one in this case, we are simply left with one node, which corresponds to $SU(2)$. By removing a simple root from the diagram, we obtain a $U(1)$ factor, so we have found the regular subalgebra $SU(2) \times U(1)$.

While this seems easy enough, a lot is happening on the algebraic level. By deleting one simple root we omit the raising and lowering operators that are associated with that root and its multiplicities. Suppose, as is done in [36], we remove the simple root α_3 . Then, only the Cartan generators H_1, H_2 survive, and the raising and lowering operators corresponding to $\alpha_2, E_{\pm\alpha_2}$, survive.

These remaining generators are:

$$H_1 = \frac{1}{2} \begin{bmatrix} 1 & 0 & 0 \\ 0 & -1 & 0 \\ 0 & 0 & 0 \end{bmatrix}, \quad H_2 = \frac{1}{2\sqrt{3}} \begin{bmatrix} 1 & 0 & 0 \\ 0 & 1 & 0 \\ 0 & 0 & -2 \end{bmatrix}, \quad (2.13)$$

$$E_{+\alpha_2} = \begin{bmatrix} 0 & 0 & 0 \\ 0 & 0 & 1 \\ 0 & 0 & 0 \end{bmatrix}, \quad E_{-\alpha_2} = \begin{bmatrix} 0 & 0 & 0 \\ 0 & 0 & 0 \\ 0 & 1 & 0 \end{bmatrix}$$

At first, the $SU(2) \times U(1)$ structure might not be clear, but after performing the following change of basis, it will be clear:

$$\begin{aligned}
t_1 &= \frac{1}{2}(E_{+\alpha_2} + E_{-\alpha_2}), \\
t_2 &= \frac{-i}{2}(E_{+\alpha_2} - E_{-\alpha_2}), \\
t_3 &= -\frac{1}{2}H_1 + \frac{\sqrt{3}}{2}H_2, \\
t_4 &= \frac{\sqrt{3}}{2}H_1 + \frac{1}{2}H_2.
\end{aligned} \tag{2.14}$$

In this new basis, the generators are:

$$t_1 = \frac{1}{2} \begin{pmatrix} 0 & 0 & 0 \\ 0 & 0 & 1 \\ 0 & 1 & 0 \end{pmatrix}, \quad t_2 = \frac{1}{2} \begin{pmatrix} 0 & 0 & 0 \\ 0 & 0 & -i \\ 0 & i & 0 \end{pmatrix}, \quad t_3 = \frac{1}{2} \begin{pmatrix} 0 & 0 & 0 \\ 0 & 1 & 0 \\ 0 & 0 & -1 \end{pmatrix}, \quad t_4 = \frac{1}{2\sqrt{3}} \begin{pmatrix} 2 & 0 & 0 \\ 0 & -1 & 0 \\ 0 & 0 & -1 \end{pmatrix}$$

Here, t_1 , t_2 , and t_3 span the Lie algebra of $SU(2)$, satisfying the usual relations, while t_4 is a generator of the $U(1)$ component, commuting with all three $SU(2)$ generators. This construction then explicitly shows how the three dimensional irrep of $SU(3)$ becomes the reducible three dimensional representation of $SU(2) \times U(1)$ and what happens when we remove a node from the Dynkin diagram. This process is relatively simple and straightforward. This works differently for special subalgebras.

There are multiple methods to finding a special subalgebra, and it often is a matter of trial and error. The first method is to look very closely at the structure of the Lie algebra itself and investigate whether we can recognise familiar structures there. This was done by [36] in detail and shall be repeated here.

To see the special subalgebra of $SU(3)$, we need to consider the three-dimensional representation **3**.

$$J_1^1 = \frac{1}{\sqrt{2}} \begin{bmatrix} 0 & 1 & 0 \\ 1 & 0 & 1 \\ 0 & 1 & 0 \end{bmatrix}, \quad J_1^2 = \frac{1}{\sqrt{2}} \begin{bmatrix} 0 & -i & 0 \\ i & 0 & -i \\ 0 & i & 0 \end{bmatrix}, \quad J_1^3 = \begin{bmatrix} 1 & 0 & 0 \\ 0 & 0 & 0 \\ 0 & 0 & -1 \end{bmatrix} \tag{2.16}$$

This representation can be written in terms of raising and lowering operators in the following way:

$$J_1^+ = \frac{J_1^1 + iJ_1^2}{\sqrt{2}}, \quad J_1^- = \frac{J_1^1 - iJ_1^2}{\sqrt{2}}, \quad H = J_3^1 \tag{2.17}$$

In the spin-1 representation, these operators can be written as matrices in the following way:

$$J_1^+ = \sqrt{2} \begin{bmatrix} 0 & 1 & 0 \\ 0 & 0 & 1 \\ 0 & 0 & 0 \end{bmatrix}, \quad J_1^- = \sqrt{2} \begin{bmatrix} 0 & 0 & 0 \\ 1 & 0 & 0 \\ 0 & 1 & 0 \end{bmatrix}, \quad H = \begin{bmatrix} 1 & 0 & 0 \\ 0 & 0 & 0 \\ 0 & 0 & -1 \end{bmatrix}. \tag{2.18}$$

This set of generators satisfies the commutation relations:

$$[H, J_1^\pm] = \pm 2J_1^\pm, \quad [J_1^+, J_1^-] = H, \tag{2.19}$$

which define the abstract algebra $\mathfrak{sl}(2)$. If one further imposes the Hermiticity conditions $H^\dagger = H$ and $(J^+)^* = J^-$, this corresponds to the compact real form $\mathfrak{su}(2)$.

These generators satisfy the $\mathfrak{su}(2)$ algebra and act irreducibly under the $SU(3)$ triplet. This irreducibility is the defining feature of the special subalgebra. In contrast, under the regular subalgebra $SU(2) \times U(1) \subset SU(3)$, the triplet reduces to $\mathbf{3} \rightarrow \mathbf{2} \oplus \mathbf{1}$. Here, a one-dimensional singlet subspace is preserved, that carries $U(1)$ charge. For the special embedding, there is no invariant subspace like that, as the entire triplet transforms under $SU(2)$ alone. Hence, the embedded $SU(2) \subset SU(3)$ forms a special subalgebra as it emerges from examining the internal structure of the representations of the Lie group.

An alternative verification method is the one we discussed in section 2.2.3. Here we follow the steps to confirm that $SU(2)$ is indeed a special subalgebra of $SU(3)$ by examining the behaviour of irreducible representations. We know that $SU(3)$ has a dimension of 8 and rank 2. $SU(2)$ has dimension 3 and rank 1. This means that $SU(2)$ is indeed a potential special subalgebra as it has a smaller dimension and rank than $SU(3)$. The next step is to see whether there is a projection matrix that projects the weights of $SU(3)$ onto the weights of $SU(2)$.

Specifically, we will examine the fundamental representation $\mathbf{3}$ of $SU(3)$. To show that $SU(2)$ is indeed a special subalgebra, we want to show that this $\mathbf{3}$ irrep of $SU(3)$ remains a three dimensional irrep for $SU(2)$. By demanding that this is the case, we can now attempt to construct and integer-valued projection matrix that maps the weights of the $\mathbf{3}$ of $SU(3)$ onto those of the $SU(2)$ representation of the same dimension.

To find the projection matrix, we need to know the weights of $SU(2)$ and $SU(3)$ of the relevant representation. We write the weights here in the Dynkin basis. The weights of the $SU(2)$ irrep of dimension $\mathbf{3}$ are $+1, -1, 0$ and the weights of the $\mathbf{3}$ irrep of $SU(3)$ are: $(1, 0), (-1, 1), (0, -1)$. Since both representations contain three weight vectors and since the rank of $SU(3)$ is 2, while that of $SU(2)$ is 1, the projection matrix must have dimensions 1×2 . If we can construct such a matrix with integer entries that maps the $SU(3)$ weights to the $SU(2)$ weights, this will provide evidence that the $SU(3)$ fundamental remains irreducible under $SU(2)$, and hence that the subalgebra is special. Now, to calculate the projection matrix, we use:

$$\begin{aligned} P(SU(3) \supset SU(2)) \begin{pmatrix} 1 \\ 0 \end{pmatrix} &= 1 \\ P(SU(3) \supset SU(2)) \begin{pmatrix} -1 \\ 1 \end{pmatrix} &= -1 \\ P(SU(3) \supset SU(2)) \begin{pmatrix} 0 \\ -1 \end{pmatrix} &= 0 \end{aligned} \tag{2.20}$$

Now, we solve the linear system to solve the 1×2 projection matrix, and we find:

$$P(SU(3) \supset SU(2)) = (1 \ 0) \tag{2.21}$$

This is an integer projection matrix, as it should be. This mapping demonstrates that

the three weights of the $SU(3)$ fundamental representation align precisely with those of the three dimensional irrep of $SU(2)$, with no splitting or multiplicities. Since the $SU(3)$ representation remains irreducible under this restriction, $SU(2)$ is confirmed to be a special subalgebra of $SU(3)$.

Now, we know that $SU(2)$ is definitely a special subalgebra, we only need to confirm that the dimensions remain the same, as a final test. To do that we use the Weyl Dimension Formula as given in section 2.6. This can be calculated by hand, but by using LieArt it was found that both representations have a dimension equal to 3, meaning that $SU(2)$ is indeed a special subalgebra of $SU(3)$ and the branching rule $\mathbf{3}_{SU(3)} \rightarrow \mathbf{3}_{SU(2)}$ is justified. This method not only works for the fundamental representation of the parent algebra, but also works for the other representations of these special cases. To show this, we will look at the following branching rule:

$$\mathbf{8}_{SU(3)} \rightarrow \mathbf{5}_{SU(2)} \oplus \mathbf{3}_{SU(2)},$$

We find the weights of the **8** representation of $SU(3)$ using LieArt, written in Dynkin notation, to be the following:

$$(1, 1), \quad (-1, 2), \quad (2, -1), \quad (0, 0), \quad (0, 0), \quad (-2, 1), \quad (1, -2), \quad (-1, -1).$$

The weights of the **5** representation of $SU(2)$ are $(2, 1, 0, -1, -2)$ and those of the **3** of $SU(2)$ again are $(1, 0, -1)$. To find the projection matrix here, we again investigate the projection of the weights. In this case, when we look at the projection:

$$P(SU(3) \supset SU(2)) \begin{pmatrix} 1 \\ 1 \end{pmatrix} = 1, \quad (2.22)$$

we already see that a possible solution for the projection matrix is

$$P = \begin{pmatrix} 1 & 1 \end{pmatrix},$$

Continuing with this projection matrix and applying it to all $SU(3)$ weights, we find that it correctly projects the **8** weights of $SU(3)$ to the combined weights of the **3 + 5** representation of $SU(2)$.

Since this integer-valued projection matrix correctly maps the $SU(3)$ weights to those of $SU(2)$, the decomposition is consistent with the embedding. However, unlike the case of the fundamental representation, here the $SU(3)$ representation does not remain irreducible under $SU(2)$ as it splits into two irreducible $SU(2)$ representations. This means that the **8** of $SU(3)$ becomes reducible under $SU(2)$, which is typical for most representations and is precisely what makes the earlier case, where the **3** stays irreducible, a sign of a special subalgebra.

The structure of the subgroups of $SU(3)$ is given in figure 2.3. Here, a dashed and straight line is drawn between $SU(2) \times U(1)$. This is because $SU(2) \times U(1)$ does not correspond to a strictly regular subalgebra in the traditional Dynkin diagram sense, since the $U(1)$ factor cannot be represented by a simple root. However, at the same time, some irreps remain irreps under this embedding, giving reason to believe there are hints for a special

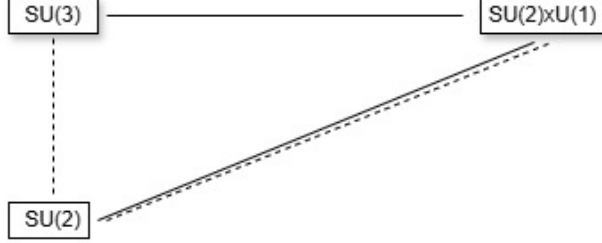


Figure 2.3: The subgroups of $SU(3)$, where the dashed line corresponds to a special subgroup and the straight line to a regular subgroup.

relationship. Since the boundary between regular and special is not this sharply defined in literature, as it is unclear whether special subalgebras are subset of regular ones or a distinct set, we treat this embedding as neither regular nor special, but some mix. This justifies the mixed line notation in the figure.

2.4 $SU(5)$

The special unitary group $SU(5)$ is a rank-4 Lie group with 24 generators and plays a big part in GUTs, particularly in the minimal $SU(5)$ GUT model, proposed by Georgi and Glashow [21]. This was the first proposal for a GUT, but however experimentally disproven, as it predicts proton decay, which has not been observed experimentally. Despite that this theory was proven incorrect, this first proposal made many researchers believe that there must be some Grand Unified Theory realised in nature. $SU(5)$ is a rank-4 group, $\mathfrak{su}(5)$ contains a 4-dimensional Cartan subalgebra.



Figure 2.4: Dynkin diagram of $SU(5)$ including its 4 simple roots.

From this Dynkin diagram, the regular subalgebras can easily be obtained by systematically removing nodes from the diagram and recognising these subalgebras. As found by [34], these regular subalgebras are:

- $SU(4) \times U(1)$
- $SU(2) \times SU(3) \times U(1)$

Now, to find the special subalgebras, we again need to use the structure of the algebra itself. By following the guide to find special subalgebras and looking at literature, we find that $Sp(4)$ is a potential special subalgebra. From the function `WeightSystem[Algebra]`

in LieArt, we find the weights of $SU(5)$ and $Sp(4)$ in the **5** representation are:

$$\begin{aligned}\lambda^{(1)} &= (1, 0, 0, 0) & \rightarrow w^{(1)} &= (0, 1) \\ \lambda^{(2)} &= (-1, 1, 0, 0) & \rightarrow w^{(2)} &= (2, -1) \\ \lambda^{(3)} &= (0, -1, 1, 0) & \rightarrow w^{(3)} &= (0, 0) \\ \lambda^{(4)} &= (0, 0, -1, 1) & \rightarrow w^{(4)} &= (-2, 1) \\ \lambda^{(5)} &= (0, 0, 0, -1) & \rightarrow w^{(5)} &= (0, -1)\end{aligned}$$

Here, the λ_i are the $SU(5)$ weights and the w_i are the $Sp(4)$ weights. Using these weights, it is found using simple calculations that the projection matrix then is:

$$P(SU(5) \supset Sp(4)) = \begin{pmatrix} 0 & 2 & 2 & 0 \\ 1 & 0 & 0 & 1 \end{pmatrix} \quad (2.23)$$

This is indeed an integer projection matrix as is expected from a subalgebra. Lastly, to test whether this is indeed a special case, we investigate the dimension of both groups. Using the function `WeylDimensionFormula[Algebra]` from LieArt for both groups and the function `HighestWeight[Algebra]` and combining these, we find that for both groups the dimension is 5. Since the dimension is equal, this must be a special subalgebra.

2.5 $SO(10)$

Another interesting group to investigate is $SO(10)$, which also contains the standard model, as: $SO(10) \subset SU(5) \subset SU(3) \times SU(2) \times U(1)$. What makes it more attractive than the $SU(5)$ model is the fact that a single 16-dimensional spinor representation of $SO(10)$ contains all fermions of one generation, including the right-handed neutrino which is not included in the $SU(5)$ models. $SO(10)$ is a special orthogonal group consisting of all 10×10 real orthogonal matrices with determinant 1, meaning that $R^T R = I$ and $\det R = 1$. This group represents rotations in ten-dimensional space and plays a key role in Grand Unified Theories (GUTs). The $SO(10)$ GUT was first proposed by Fritzsch and Minkowski in 1975 [20], making it one of the earliest unified theories beyond $SU(5)$. Unlike $SU(5)$, $SO(10)$ has not been experimentally ruled out.

The group $SO(10)$ is compact, simple, and of rank 5, with a total of $\dim(SO(10)) = \frac{10(10-1)}{2} = 45$ generators. These generators form the Lie algebra $\mathfrak{so}(10)$, which consists of real, antisymmetric 10×10 matrices.

$SO(10)$ is of rank 5, with a Cartan subalgebra consisting of five commuting generators H_1, \dots, H_5 . The root system of $\mathfrak{so}(10)$ is formed by the eigenvalues of the adjoint action of these generators on the other elements of the Lie algebra [24].

The Dynkin diagram of $SO(10)$ consists of 5 simple roots as can be seen in figure 2.6.

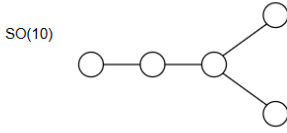


Figure 2.5: Dynkin diagram of $SO(10)$, containing 5 simple roots.

The regular subgroups can now easily be obtained by removing nodes from the diagram. The following ones are named in [34]:

- $SU(5) \times U(1)$,
- $SU(4) \times SU(2) \times SU(2)$ The Pati-Salam group provides an alternative symmetry-breaking route to the Standard Model, where the $SU(4)$ treats leptons as the fourth colour [7],
- $SO(8) \times U(1)$,

Now, for special subalgebras, a similar method as discussed in section 2.3 can be performed where we follow the guide from section 2.2.3. By doing this and finding the possible subalgebras with representation equal to that of the representation of the algebra, we find the special subalgebras, as found by [34]. These are the following:

- $Sp(4)$,
- $SO(9)$,
- $Sp(4) \times Sp(4)$,
- $SU(2) \times SO(7)$.

Figure 2.6, summarises all these regular and special subalgebras of $SO(10)$ up until $SU(2)$.

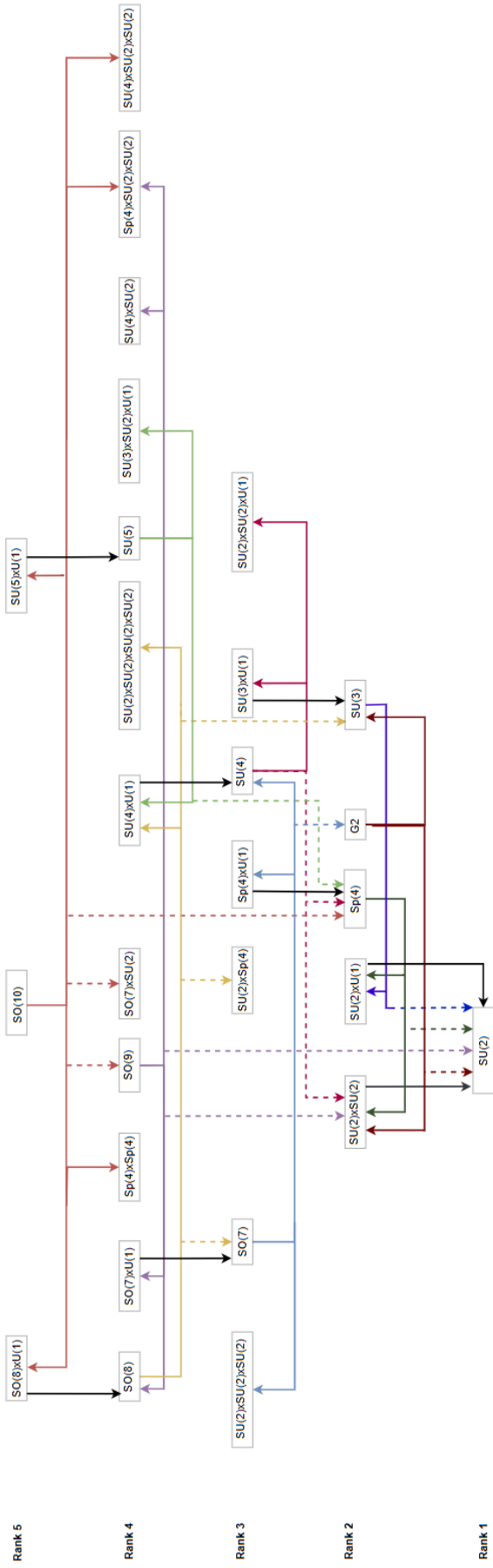


Figure 2.6: All groups corresponding to the regular (straight line) and special (dotted line) of $SO(10)$ [34].

Chapter 3

VEVs of Continuous Groups

Now that we have discovered how to find all continuous subalgebras, it is time to move onto the next step, which is assigning the VEVs to the breaking of the continuous symmetries. The Vacuum Expectation Value (VEV) is the average value of a quantum field in its vacuum state: $\langle \phi \rangle = v$. A zero VEV means that the vacuum state respects the full symmetry of the Lagrangian, meaning that there is no spontaneous symmetry breaking. A non-zero VEV indicates that the vacuum state does not share the full symmetry of the Lagrangian and thus that the symmetry is spontaneously broken [31]. To show how this happens, we will look into the example of the Higgs doublet for the breaking of $SU(2)_L \times U(1)_Y$. Here, L stands for "left", referring to the fact that the $SU(2)_L$ acts only on left-handed fermions. The Y stands for hypercharge, the quantum number associated with the $U(1)_Y$ gauge group. The generator of electromagnetism, denoted as Q , will emerge as a specific combination of the electroweak generators. We will derive this relation when studying the effect of the VEV on the gauge symmetry.

3.1 $SU(2) \times U(1)$

3.1.1 Higgs doublet

In the following example, we want to introduce a single scalar field ϕ with a vacuum expectation value $\langle \phi \rangle$ such that we obtain the following symmetry breaking pattern:

$$SU(2)_L \times U(1)_Y \xrightarrow{\langle \phi \rangle} U(1)_{EM} \quad (3.1)$$

For this symmetry breaking, we need a complex scalar doublet to break the $SU(2)$ symmetry. Besides this, we also need one part of the doublet to be neutral to have a possibility to obtain a $U(1)_{EM}$ symmetry. So, we need the following complex doublet:

$$\Phi = \begin{pmatrix} \phi^+ \\ \phi^0 \end{pmatrix}, Y(\Phi) = 1. \quad (3.2)$$

The theory must then be constructed in such a way that the vacuum is invariant under a $U(1)_Q$ gauge, but not under $SU(2)_L \times U(1)_Y$. An example of such a scalar potential is the

so-called Mexican hat potential:

$$V(\phi) = -\mu^2 \phi^\dagger \phi + \lambda(\phi^\dagger \phi)^2 \quad (3.3)$$

Here, μ and λ are real constants. Now, to determine ϕ , we need to find the minimum for $V(\phi)$. While for $\lambda < 0$ the potential is unphysical, for $\lambda > 0$, it obtains a minimum for,

$$\phi^\dagger \phi = \frac{\mu^2}{2\lambda} \equiv \frac{v^2}{2} \quad (3.4)$$

Then, the VEV is:

$$\langle \phi \rangle = \frac{1}{\sqrt{2}} \begin{pmatrix} 0 \\ v \end{pmatrix}, v^2 = \frac{\mu^2}{\lambda} \quad (3.5)$$

The specific form of $\langle \phi \rangle$ is a gauge choice, which means that we can always rotate any solution of this form using $SU(2)$ symmetry, but this form is usually picked. With this VEV, the $SU(2)_L \times U(1)_Y$ is spontaneously broken into $U(1)_{EM}$.

To understand the consequences of this VEV on the gauge fields, we examine the covariant derivative term in the Lagrangian:

$$\mathcal{L}_{\text{kinetic}} = (D_\mu \phi)^\dagger (D^\mu \phi), \quad (3.6)$$

where the covariant derivative is defined as:

$$D_\mu \phi = (\partial_\mu - \frac{ig}{2} \tau^a W_\mu^a - \frac{ig'}{2} B_\mu) \phi, \quad (3.7)$$

with g and g' the gauge couplings of $SU(2)_L$ and $U(1)_Y$ respectively, τ^a the Pauli matrices, W_μ^a the gauge bosons for $SU(2)$ and B_μ the gauge boson for $U(1)$. Substituting the VEV into this expression gives rise to mass terms for the gauge fields:

$$(D_\mu \langle \phi \rangle)^\dagger (D^\mu \langle \phi \rangle) = \frac{v^2}{8} [g^2 |W_\mu^1 - iW_\mu^2|^2 + |gW_\mu^3 - g'B_\mu|^2]. \quad (3.8)$$

To identify the physical fields, we define the charged combinations of the vector bosons:

$$W_\mu^\pm = \frac{1}{\sqrt{2}} (W_\mu^1 \mp iW_\mu^2), \quad (3.9)$$

which yield the W -boson mass term: $m_W = \frac{gv}{2}$. The remaining neutral fields W_μ^3 and B_μ mix to form the massive state:

$$Z_\mu^0 = \frac{1}{\sqrt{g^2 + g'^2}} (gW_\mu^3 - g'B_\mu), \quad (3.10)$$

which obtains the Z -boson mass term: $m_Z = \frac{v}{2} \sqrt{g^2 + g'^2}$.

Besides the Z boson, the mixing of the neutral fields also form the massless vector boson:

$$A_\mu = \frac{g'W_\mu^3 + gB_\mu}{\sqrt{g^2 + g'^2}} \quad (3.11)$$

This boson corresponds to the photon.

Thus, out of the original four generators of $SU(2)_L \times U(1)_Y$, three are broken and give mass to the W^\pm and Z bosons, while one unbroken generator gives rise to the massless photon of $U(1)_{EM}$.

This structure also reveals the presence of Goldstone bosons. According to the Goldstone theorem, for each broken generator of a continuous global symmetry, a massless scalar particle, a Goldstone boson, should appear. In the case of gauge theories such as the Standard Model, these Goldstone bosons are 'eaten' by the gauge bosons, becoming their longitudinal components and giving them mass. This is the essence of the Higgs mechanism.

We can determine the unbroken generator after spontaneous symmetry breaking by examining which linear combination of the original generators leaves the Higgs vacuum invariant. Consider a general infinitesimal transformation under the continuous symmetry group $SU(2)$:

$$\phi \rightarrow \phi' = (1 + i\alpha^a T^a + i\beta Y) \phi, \quad (3.12)$$

where $T^a = \frac{1}{2}\sigma^a$ are the generators of $SU(2)_L$, Y is the hypercharge generator of $U(1)_Y$, and $\alpha^a, \beta \in \mathbb{R}$ are infinitesimal parameters. We want to find a linear combination of generators

$$\hat{Q} = \alpha^a T^a + \beta Y \quad (3.13)$$

such that

$$\hat{Q}\langle\phi\rangle = 0, \quad (3.14)$$

such that the VEV is invariant under this transformation.

We again use the Higgs doublet from before:

$$\langle\phi\rangle = \frac{1}{\sqrt{2}} \begin{pmatrix} 0 \\ v \end{pmatrix}. \quad (3.15)$$

We now apply each generator to $\langle\phi\rangle$:

$$T^1\langle\phi\rangle = \frac{1}{2} \begin{pmatrix} v \\ 0 \end{pmatrix}, \quad T^2\langle\phi\rangle = -\frac{i}{2} \begin{pmatrix} v \\ 0 \end{pmatrix}, \quad T^3\langle\phi\rangle = -\frac{1}{2} \begin{pmatrix} 0 \\ v \end{pmatrix}, \quad Y\langle\phi\rangle = \begin{pmatrix} 0 \\ v \end{pmatrix}.$$

So a linear combination $\hat{Q} = \alpha^a T^a + \beta Y$ acts as:

$$\hat{Q}\langle\phi\rangle = (\alpha^1 T^1 + \alpha^2 T^2 + \alpha^3 T^3 + \beta Y) \langle\phi\rangle = \left(\frac{v}{2} (\alpha^1 - i\alpha^2) \begin{pmatrix} 1 \\ 0 \end{pmatrix} + v \left(-\frac{\alpha^3}{2} + \beta \right) \begin{pmatrix} 0 \\ 1 \end{pmatrix} \right). \quad (3.16)$$

For this to vanish, both components must be zero. This gives:

$$\alpha^1 - i\alpha^2 = 0 \quad \Rightarrow \quad \alpha^1 = \alpha^2 = 0,$$

and

$$-\frac{\alpha^3}{2} + \beta = 0 \quad \Rightarrow \quad \beta = \frac{\alpha^3}{2}.$$

Hence, the only infinitesimal transformation that leaves the VEV invariant is:

$$\hat{Q} = \alpha^3 T^3 + \frac{\alpha^3}{2} Y = \alpha^3 \left(T^3 + \frac{Y}{2} \right). \quad (3.17)$$

Therefore, the unbroken generator is:

$$Q = T_3 + \frac{Y}{2}, \quad (3.18)$$

which defines the electromagnetic charge operator in the electroweak theory.

3.1.2 Different VEVs

Having established the Higgs doublet mechanism for $SU(2)_L \times U(1)_Y$, we now explore alternative choices for the scalar field representation and VEV. These choices can lead to different patterns of spontaneous symmetry breaking, potentially leaving other subgroups unbroken or fully breaking the original symmetry.

Studying such alternative VEVs is not only of theoretical interest, but also relevant in the context of Beyond the Standard Model (BSM) physics and (GUTs), where scalar fields in different representations may be used to trigger more complex breaking patterns. In particular, we will investigate the consequences of assigning VEVs to scalar fields in other representations of $SU(2)_L \times U(1)_Y$, such as the triplet $(3, 0)$ or the singlet $(1, 1)$, and determine the resulting unbroken subgroups.

This analysis allows us to understand how the structure of the scalar representation and the direction of the VEV determine which generators are preserved, and whether any $U(1)$ subgroup survives.

- $\phi \sim (3, 0)$

Here, we are dealing with a triplet representation, which is the adjoint representation of $SU(2)$, and the hypercharge $Y = 0$. In the triplet representation, the generators L_a are 3×3 matrices defined in the following way:

$$L_1 = \begin{pmatrix} 0 & 0 & 0 \\ 0 & 0 & -i \\ 0 & i & 0 \end{pmatrix}, L_2 = \begin{pmatrix} 0 & 0 & i \\ 0 & 0 & 0 \\ -i & 0 & 0 \end{pmatrix}, L_3 = \begin{pmatrix} 0 & -i & 0 \\ i & 0 & 0 \\ 0 & 0 & 0 \end{pmatrix} \quad (3.19)$$

Suppose now we choose the VEV $\langle \phi \rangle = \begin{pmatrix} 0 \\ 0 \\ v \end{pmatrix}$ and act with the infinitesimal transformation:

$$\phi \rightarrow \phi' = (1 + i\alpha_a L^a) \phi. \quad (3.20)$$

Now, we want to see again which generator remains unbroken.

$$\begin{aligned}
L_1 \begin{pmatrix} 0 \\ 0 \\ v \end{pmatrix} &= \begin{pmatrix} 0 \\ -iv \\ 0 \end{pmatrix} \neq \begin{pmatrix} 0 \\ 0 \\ 0 \end{pmatrix} \Rightarrow \text{broken} \\
L_2 \begin{pmatrix} 0 \\ 0 \\ v \end{pmatrix} &= \begin{pmatrix} iv \\ 0 \\ 0 \end{pmatrix} \neq \begin{pmatrix} 0 \\ 0 \\ 0 \end{pmatrix} \Rightarrow \text{broken} \\
L_3 \begin{pmatrix} 0 \\ 0 \\ v \end{pmatrix} &= \begin{pmatrix} 0 \\ 0 \\ 0 \end{pmatrix} \Rightarrow \text{invariant}
\end{aligned} \tag{3.21}$$

So, there is again only one unbroken generator, L_3 , meaning that the only symmetry that remains is generated by L_3 and that is $U(1)$. This means that $SU(2)_L \times U(1)_Y \rightarrow U(1)_{T^3}$ and for the electric charge operator $Q = T_3$, since $Y = 0$.

- $\phi \sim (3, 1)$

In this case we are dealing with a similar case as before but now with a hypercharge $Y = 1$. This gives us the following infinitesimal transformation:

$$\phi \rightarrow \phi' = (1 + i\alpha_a L^a + i\beta Y) \phi$$

where we can use the results of equation 3.21. When we multiply the hypercharge with the VEV, we find

$$Y\langle\phi\rangle = \begin{pmatrix} 0 \\ 0 \\ v \end{pmatrix}.$$

We must now solve

$$(\alpha_3 L^3 + \beta Y)\langle\phi\rangle = 0. \tag{3.22}$$

However,

$$L^3\langle\phi\rangle = 0$$

so we get:

$$\beta\langle\phi\rangle = 0 \Rightarrow \beta = 0. \tag{3.23}$$

This means that again only T^3 is the unbroken generator and the residual symmetry is $U(1)_{T^3}$.

- $\phi \sim (1, 1)$

In this case we are dealing with a singlet under $SU(2)_L$ and a hypercharge $Y = 1$. We choose the VEV $\langle\phi\rangle = v$. Since we are dealing with a singlet, $T^a\phi = 0$, so the only action comes from the hypercharge:

$$(\alpha_a T^a + \beta Y)\langle\phi\rangle = \beta Y\langle\phi\rangle = \beta v \tag{3.24}$$

This only vanishes for $\beta = 0$. So, in this case, all T^a are unbroken generators, meaning that the symmetry that remains is $SU(2)_L$.

- $\phi \sim (2, 0)$

Here, we are dealing with a doublet again and a hypercharge $Y = 0$. We choose the VEV $\begin{pmatrix} 0 \\ v \end{pmatrix}$ and let it act on the matrices T_a , as before with the Higgs doublet case, but without the hypercharge. This means that there is no non-trivial combination of $SU(2)$ generators to leave the VEV invariant, so all $\alpha_a = 0$. This means that all generators are broken and the residual symmetry is simply the trivial group $\{e\}$.

After having seen how different VEVs give different results for the breaking of the group $SU(2)_L \times U(1)_Y$, we can look at the VEVs of other groups.

3.2 $SU(3)$

The logical next group to investigate is $SU(3)$, which has two possible maximal subgroups, $SU(2) \times U(1)$ and $SU(2)$, as we have established in section 2.3. In what follows, we will analyse several scalar representations of $SU(3)$ — such as the fundamental **3** and adjoint **8** — and determine how different VEV choices affect the symmetry breaking pattern. We will again make use of infinitesimal transformations to identify which generators leave the VEV invariant and thereby identify the unbroken subgroup. The logic will mirror our approach in the $SU(2)_L \times U(1)_Y$ case: by explicitly acting with the generators of $SU(3)$ on the chosen VEV and checking which combinations annihilate it, we determine the residual symmetry.

In order to break the Lie group G to a subgroup H via a VEV, the scalar field acquiring said VEV must transform in a representation of G that contains an H -singlet. This in turn ensures that the VEV is invariant under the action of H and then makes sure to preserve the subgroup. If there is no singlet in the decomposition of the representation under H , the VEV breaks the whole parent group, including the subgroup H . So, keeping this criterion in mind, we continue our investigation into the VEVs for breaking the $SU(3)$ symmetry into subgroups.

By using LieArt, we have found that the **6**-representation of $SU(3)$ is the smallest representation that contains an $SU(2)$ singlet, as can be seen in table 3.2 [18].

$SU(3)$ rep.	$SU(2)$ decomposition
3	3
6	1 + 5
8	3 + 5
10	3 + 7
15	3 + 5 + 7
21	3 + 7 + 11
27	1 + 2(5) + 7 + 9

Table 3.1: Branching rules of $SU(3) \supset SU(2)$ [17].

Using another Mathematica extension, GroupMath [19], we can also very easily find the generators of these representations. By simply using the function `MatrixForm` /@ `RepMatrices[Algebra, representation]` and filling in the relevant algebra and representation, we find the generators of the representation. For the **6** representation, these are the following:

$$\begin{aligned}
T^1 &= \begin{bmatrix} 0 & -\frac{1}{\sqrt{2}} & 0 & 0 & 0 & 0 \\ -\frac{1}{\sqrt{2}} & 0 & 0 & -\frac{1}{\sqrt{2}} & 0 & 0 \\ 0 & 0 & 0 & 0 & -\frac{1}{2} & 0 \\ 0 & -\frac{1}{\sqrt{2}} & 0 & 0 & 0 & 0 \\ 0 & 0 & -\frac{1}{2} & 0 & 0 & 0 \\ 0 & 0 & 0 & 0 & 0 & 0 \end{bmatrix}, \\
T^2 &= \begin{bmatrix} 0 & -\frac{i}{\sqrt{2}} & 0 & 0 & 0 & 0 \\ \frac{i}{\sqrt{2}} & 0 & 0 & -\frac{i}{\sqrt{2}} & 0 & 0 \\ 0 & 0 & 0 & 0 & -\frac{i}{2} & 0 \\ 0 & \frac{i}{\sqrt{2}} & 0 & 0 & 0 & 0 \\ 0 & 0 & \frac{i}{2} & 0 & 0 & 0 \\ 0 & 0 & 0 & 0 & 0 & 0 \end{bmatrix}, \\
T^3 &= \begin{bmatrix} -1 & 0 & 0 & 0 & 0 & 0 \\ 0 & 0 & 0 & 0 & 0 & 0 \\ 0 & 0 & -\frac{1}{2} & 0 & 0 & 0 \\ 0 & 0 & 0 & 1 & 0 & 0 \\ 0 & 0 & 0 & 0 & \frac{1}{2} & 0 \\ 0 & 0 & 0 & 0 & 0 & 0 \end{bmatrix}, \\
T^4 &= \begin{bmatrix} 0 & 0 & -\frac{1}{\sqrt{2}} & 0 & 0 & 0 \\ 0 & 0 & 0 & 0 & -\frac{1}{2} & 0 \\ -\frac{1}{\sqrt{2}} & 0 & 0 & 0 & 0 & -\frac{1}{\sqrt{2}} \\ 0 & 0 & 0 & 0 & 0 & 0 \\ 0 & -\frac{1}{2} & 0 & 0 & 0 & 0 \\ 0 & 0 & -\frac{1}{\sqrt{2}} & 0 & 0 & 0 \end{bmatrix}, \\
T^5 &= \begin{bmatrix} 0 & 0 & -\frac{i}{\sqrt{2}} & 0 & 0 & 0 \\ 0 & 0 & 0 & 0 & -\frac{i}{2} & 0 \\ \frac{i}{\sqrt{2}} & 0 & 0 & 0 & 0 & -\frac{i}{\sqrt{2}} \\ 0 & 0 & 0 & 0 & 0 & 0 \\ 0 & \frac{i}{2} & 0 & 0 & 0 & 0 \\ 0 & 0 & \frac{i}{\sqrt{2}} & 0 & 0 & 0 \end{bmatrix}, \\
T^6 &= \begin{bmatrix} 0 & 0 & 0 & 0 & 0 & 0 \\ 0 & 0 & -\frac{1}{2} & 0 & 0 & 0 \\ 0 & -\frac{1}{2} & 0 & 0 & 0 & 0 \\ 0 & 0 & 0 & 0 & -\frac{1}{\sqrt{2}} & 0 \\ 0 & 0 & 0 & -\frac{1}{\sqrt{2}} & 0 & -\frac{1}{\sqrt{2}} \\ 0 & 0 & 0 & 0 & -\frac{1}{\sqrt{2}} & 0 \end{bmatrix},
\end{aligned}$$

$$T^7 = \begin{bmatrix} 0 & 0 & 0 & 0 & 0 & 0 \\ 0 & 0 & -\frac{i}{2} & 0 & 0 & 0 \\ 0 & \frac{i}{2} & 0 & 0 & 0 & 0 \\ 0 & 0 & 0 & 0 & -\frac{i}{\sqrt{2}} & 0 \\ 0 & 0 & 0 & \frac{i}{\sqrt{2}} & 0 & -\frac{i}{\sqrt{2}} \\ 0 & 0 & 0 & 0 & \frac{i}{\sqrt{2}} & 0 \end{bmatrix},$$

$$T^8 = \begin{bmatrix} -\frac{1}{\sqrt{3}} & 0 & 0 & 0 & 0 & 0 \\ 0 & -\frac{1}{\sqrt{3}} & 0 & 0 & 0 & 0 \\ 0 & 0 & \frac{1}{2\sqrt{3}} & 0 & 0 & 0 \\ 0 & 0 & 0 & -\frac{1}{\sqrt{3}} & 0 & 0 \\ 0 & 0 & 0 & 0 & \frac{1}{2\sqrt{3}} & 0 \\ 0 & 0 & 0 & 0 & 0 & \frac{2}{\sqrt{3}} \end{bmatrix}$$

With these generators and the branching rule

$$\mathbf{6} \rightarrow \mathbf{1} \oplus \mathbf{5},$$

from table 3.2, we can figure out which unbroken groups and generator this representation leads

to. We choose the VEV $\begin{pmatrix} 0 \\ 0 \\ 0 \\ 0 \\ 0 \\ v \end{pmatrix}$ and apply this VEV to the **6** generators.

The results, obtained in Mathematica, are:

$$T^1\langle\phi\rangle = \begin{pmatrix} 0 \\ 0 \\ 0 \\ 0 \\ 0 \\ 0 \end{pmatrix}, \quad T^2\langle\phi\rangle = \begin{pmatrix} 0 \\ 0 \\ 0 \\ 0 \\ 0 \\ 0 \end{pmatrix}, \quad T^3\langle\phi\rangle = \begin{pmatrix} 0 \\ 0 \\ 0 \\ 0 \\ 0 \\ 0 \end{pmatrix},$$

$$T^4\langle\phi\rangle = \begin{pmatrix} 0 \\ 0 \\ -\frac{v}{\sqrt{2}} \\ 0 \\ 0 \\ 0 \end{pmatrix}, \quad T^5\langle\phi\rangle = \begin{pmatrix} 0 \\ 0 \\ -\frac{iv}{\sqrt{2}} \\ 0 \\ 0 \\ 0 \end{pmatrix}, \quad T^6\langle\phi\rangle = \begin{pmatrix} 0 \\ 0 \\ 0 \\ 0 \\ -\frac{v}{\sqrt{2}} \\ 0 \end{pmatrix},$$

$$T^7\langle\phi\rangle = \begin{pmatrix} 0 \\ 0 \\ 0 \\ 0 \\ -\frac{iv}{\sqrt{2}} \\ 0 \end{pmatrix}, \quad T^8\langle\phi\rangle = \begin{pmatrix} 0 \\ 0 \\ 0 \\ 0 \\ 0 \\ \frac{2v}{\sqrt{3}} \end{pmatrix}.$$

We observe that the first three generators T^1, T^2, T^3 annihilate the VEV. Here we are considering only the real Hermitian generators T^a themselves. We do not permit the linear complex combinations such as $T^4 + iT^5$. This implies that the VEV is invariant under the action of these three generators. These are precisely the generators of the Lie algebra $\mathfrak{su}(2)$ embedded inside $\mathfrak{su}(3)$.

Physically, this means that the symmetry associated with T^1, T^2, T^3 is unbroken. The remaining five generators do not annihilate the VEV and thus correspond to broken symmetries, generating five Goldstone bosons.

Conclusion: The VEV in the singlet direction of the **6** representation breaks the symmetry as:

$$SU(3) \rightarrow SU(2),$$

with $SU(2)$ generated by the unbroken generators T^1, T^2, T^3 .

Now, we can do the same for the generators of **27**. This has the branching rule

$$\mathbf{27} \rightarrow \mathbf{9} \oplus \mathbf{7} \oplus \mathbf{2(5)} \oplus \mathbf{1}$$

For this representation we will choose the VEV $\begin{pmatrix} 0 \\ 0 \\ \vdots \\ 0 \\ v \end{pmatrix}$, where the v is at the last position of the vector.

When multiplying the generators of the **27** representation with this VEV, we find that the only unbroken generators are T^1, T^2, T^3 and T^8 . The generators T^1, T^2, T^3 form the $SU(2)$ subgroup and annihilate the VEV. The generator T^8 , the second Cartan generator of $SU(3)$, also annihilates the VEV and corresponds to $U(1)$. This means that the VEV preserves the subgroup generated by $\{T^1, T^2, T^3, T^8\}$ corresponds to $SU(2) \times U(1)$. This confirms the breaking pattern we discussed in section 2.3.

Now, that we have the VEVs of the $SU(3)$ maximal breaking patterns, we can move on to the next group of our interest, $SO(10)$.

3.3 $SO(10)$

The breaking patterns of $SO(10)$ are particularly of interest to us, as this group is a possible GUT. Since the Standard Model alone is not able to explain all the physical phenomena we see in nature, we need a larger symmetry, a GUT, to explain these missing parts of the Standard Model. The first GUT put forth by Glashow and Georgi in [21] was $SU(5)$. However, $SU(5)$ has been experimentally ruled out as a GUT, because of its proton decay prediction. This GUT predicts a proton lifetime much shorter than we see in nature.

The next possible smallest, simple Lie group to contain the Standard Model is $SO(10)$. This group offers the advantage that all fermions of one generation fit into a singlet 16-dimensional spinor representation. The critical question here is whether the commonly assumed breaking chains such as $SO(10) \rightarrow SU(5) \rightarrow \text{SM}$ or $SO(10) \rightarrow SU(4) \times SU(2) \times SU(2) \rightarrow \text{SM}$, actually minimise the vacuum energy. Researchers typically assume this breaking pattern without verification, but the

actual symmetry-breaking chain is determined by whichever scalar field minimised the potential. As we will see in this subchapter, there are many other breaking paths in $SO(10)$ to follow, besides the one to the Standard Model. All of these are allowed in group theory and may be energetically preferred for certain parameter values.

In this research, we calculate the VEVs of all maximal subgroups of $SO(10)$ and provide a clear framework on how to calculate them. This way, future researchers are able to determine all the VEVs of all of the $SO(10)$ symmetry breaking chains, such that they can calculate all of their energy minima. This way, it can be decided which breaking pattern is preferred. Our classification of VEVs enables future researchers to do comprehensive numerical scans of the whole parameter space, such as the ones done by Magnus Petz, which are discussed in section 3.3.2.

For the VEVs of $SO(10)$ we look at the work found in literature [8], [9], [10], [25], [39]. In the work done by Held, Kwapisz and Sartore we find the VEVs of multiple breaking chains of $SO(10)$ [23]. In this work, group-theoretical analysis is combined with a study of the scalar potential. Besides the VEVs found in this work, we will also use Mathematica. In table 3.2, for each maximal subgroup of $SO(10)$ we list, first the smallest irreducible representation of $SO(10)$ that contains a singlet under that subgroup, and secondly an explicit form of the vacuum expectation value in that representation. To determine these smallest irreps, we use the $SO(10)$ branching rules found in table 41 of [34] and in [17]. These branching rules could also be derived using projection matrices, however since they are readily available in literature, we simply reference these findings.

Suppose you were interested in a subgroup that is not easily found in literature, such as the non-maximal subgroups, the projection matrix can be found using the method described in 2.2.1. Using this method, we build a projection matrix P that maps the weights of the $SO(10)$ representation onto those of the subgroup we are interested in. By applying P to all the weights of the original $SO(10)$ representation we find the projected weights. These projected weights then fall into sets that you can recognise as certain representations of the subgroup. This way the branching rules can be found algebraically. Programs such as Lie Art [18] and GroupMath [19] can also be used for this.

Up until now we have only presented VEVs as vectors, but in table 3.2, there are also matrices used. This is because the form of the VEV depends on the representation space of the group. The fundamental representation **(10)** of $SO(10)$ acts on vectors in \mathbb{R}^{10} , meaning that the representation space is made of 10-component vectors. In this case, the VEV is a vector as can be seen for the $SO(9)$ subgroup.

The adjoint representation **(45)** however, is given by the Lie algebra, which consists of skew-symmetric 10×10 matrices. This means that the VEV corresponding to this representation must also be an skew-symmetric matrix. The **54** representation arises in the decomposition: $10 \otimes 10 = 1' \oplus 45 \oplus 54$. Here the **54** corresponds to the symmetric, traceless part of the tensor product. Since the tensor product of $10 \otimes 10$ consists of rank-2 tensors, the **54** field is represented by a symmetric and traceless 10×10 matrix. Its VEV must therefore take matrix form.

In these cases where the representations of $SO(10)$ consists of matrices, the VEV can be simplified by an appropriate $SO(10)$ basis transformation. In [32] it is shown that any skew-symmetric $2n \times 2n$ matrix can be transformed under $SO(2n)$ into a block-diagonal form, given by

$$\phi = \text{diag}(l_1 J, \dots, l_n J), \quad (3.25)$$

where

$$J = \begin{pmatrix} 0 & 1 \\ -1 & 0 \end{pmatrix}. \quad (3.26)$$

The real parameters l_i are the independent invariants of the antisymmetric matrix under conjugation. The same work shows that this block-diagonal form is equivalent to an antidiagonal skew-symmetric matrix through another change of basis. Since VEVs related by any $SO(10)$ transformation are physically equivalent, we choose this antidiagonal block form for the **45** as can be seen in table 3.2.

On the other hand, the **54** transforms as symmetric, traceless 10×10 matrices. Any symmetric matrix can easily be diagonalised by an orthogonal transformation, so an $SO(10)$ transformation. This is why in table 3.2, the VEVs for the **54** are diagonalised.

Subgroup of $SO(10)$	Representation	VEV
$SO(9)$	10	$(0, 0, 0, 0, 0, 0, 0, 0, 0, v)$
$SO(8) \times U(1)$	45	Antidiag($-w_8, 0, 0, 0, 0, 0, 0, 0, 0, w_8$)
$SO(7) \times SU(2)$	54	Diag($\frac{7}{3}, \frac{7}{3}, \frac{7}{3}, -1, -1, -1, -1, -1, -1$)
$SU(5) \times U(1)$	45	Antidiag($v, v, v, v, v, -v, -v, -v, -v, -v$)
$Sp(4) \times Sp(4)$	54	Diag($v, v, v, v, v, -v, -v, -v, -v, -v$)
$SU(4) \times SU(2) \times SU(2)$	54	Diag($\frac{3}{5}, \frac{3}{5}, \frac{3}{5}, \frac{3}{5}, -\frac{2}{5}, -\frac{2}{5}, -\frac{2}{5}, -\frac{2}{5}, -\frac{2}{5}$)
$Sp(4)$	120	Diag($0, \dots, 0, \underbrace{v, v, v, v, v, v, v, v, v}_{\text{positions 57-64}}, 0, \dots, 0$)

Table 3.2: VEVs corresponding to different subgroup embeddings of $SO(10)$. The representation column corresponds to the lowest representation where the relevant subgroup obtains a singlet when breaking $SO(10)$. The VEVs for the subgroups $SO(8) \times U(1)$ and $SU(5) \times U(1)$ were found in [23]. In this work by Held et al. an $SO(10)$ model is studied with scalar content $\mathbf{16}_H \oplus \mathbf{45}_H$. The listed VEVs are for the $\mathbf{45}_H$ alone, which is sufficient to break $SO(10)$ to these intermediate symmetries. The $\mathbf{16}_H$ representation can then acquire additional VEVs to break further to the Standard Model. The VEVs for $SO(7) \times SU(2)$ was found in [13] and the VEV for $SU(4) \times SU(2) \times SU(2)$ was found in [7]. The others were found using Mathematica [37].

The VEVs not found in literature were found using Mathematica, which code will be explained here. The VEVs found in literature were used to check the validity of proper functionality of the code. To find the VEVs for the different subgroups of $SO(10)$, we will go through the method used.

3.3.1 Methodology for finding VEV textures

First of all, we construct the generator matrices of $\mathfrak{so}(10)$ in the fundamental (**10**) representation. To do this, we make use of the fact that this algebra consists of all real, antisymmetric 10×10 matrices. The full set of generators can then be systematically defined by creating for each distinct

index pair (a, b) (where $a < b$) a matrix whose (a, b) -entry is $-i$, each (b, a) -entry is i and the other entries are zero. This process can then be implemented in Mathematica by looping over all entry pairs (a, b) . The exact code can be found below. This produces a list of 45 matrices, which forms a basis of the fundamental representation of the $\mathfrak{so}(10)$ Lie algebra. Higher-dimensional representations like the **45** and **54** are then obtained from the fundamental generators by using the relevant tensor-products.

Listing 3.1: Initialisation of $SO(10)$ generators

```

n=10
(* Initialise list of generators *)
so10Generators =
  Table[Module[{gen = ConstantArray[0, {n, n}]}, gen[[a, b]] = -I;
  gen[[b, a]] = I;
  gen], {a, 1, n}, {b, a + 1, n}] // Flatten[#, 1] &;

```

In the previous subchapter we used GroupMath to find the generators of the representations. While this worked well for $SU(3)$, it did not give the right generators for our VEVs. GroupMath chooses a basis in which as many generators as possible are diagonal. This is convenient for complex representations, but not ideal for our thesis. In this work we represent $\mathfrak{so}(10)$ in the usual Hermitian convention by imaginary antisymmetric matrices. In such an imaginary antisymmetric basis, there can be no nontrivial diagonal generator. So, the matrices produced by GroupMath do not match the basis in which we construct our VEVs.

Now that we have the necessary generators, we will define a candidate VEV. To do this we combine trial and error and critical thinking. First we take a look at the relevant representation. For $SO(9)$, the relevant representation is the fundamental one (**10**), as this results in a singlet for this subgroup according to the $SO(10)$ branching rules in [18]. This means that for this subgroup, our VEV will live in the vector representation and must therefore be an ordinary 10-component vector. For $SO(7) \times SU(2)$, $Sp(4) \times Sp(4)$ and $SU(4) \times SU(2) \times SU(2)$, **54** is the relevant representation at which all these subgroups attain a singlet in the symmetry breaking. The $SO(10)$ relation $10 \otimes 10 = 1' \oplus 45 \oplus 54$ shows that the **54** corresponds to the symmetric traceless part of the rank-2 tensor product $10 \otimes 10$. Any symmetric matrix in $SO(10)$ can be diagonalised by an $SO(10)$ basis transformation. Therefore, a VEV in the **54** can always be taken to be a diagonal traceless matrix.

We have a similar case for the **45**, which is relevant for $SU(5) \times U(1)$ and $SO(8) \times U(1)$, which are covered in [23]. This representation corresponds to the antisymmetric part of $10 \otimes 10$. VEVs in the **45** can therefore be written as antisymmetric matrices and can be simplified to antidiagonal form, as explained earlier.

This means that except for $Sp(4)$, we can simply use 10×10 traceless, diagonal matrices for the VEV. Now, we need to propose trials VEVs, that are consistent with the group's representation structure. To do this, we need to look at the branching rules of each individual subgroup. Let's take the subgroup $SU(4) \times SU(2) \times SU(2)$ as our example. Under this subgroup, $10 = (1, 2, 2) + (6, 1, 1)$. Now, the label $(1, 2, 2)$ means that the dimension of this subspace is four, as $1 \times 2 \times 2 = 4$. The label $(6, 1, 1)$ means that the dimension of the subspace is six. From the traceless condition, we can then immediately obtain the following VEV:

$$\langle \phi \rangle = \text{diag}\left(\frac{3}{5}, \frac{3}{5}, \frac{3}{5}, \frac{3}{5}, -\frac{2}{5}, -\frac{2}{5}, -\frac{2}{5}, -\frac{2}{5}, -\frac{2}{5}, -\frac{2}{5}\right) \quad (3.27)$$

Now, to prove that this VEV is indeed correct, we need to confirm that the VEV leaves the correct amount of unbroken generators associated to the subgroup. To do this, we implement a simple code into Mathematica in which we use the commutator relation to find the amount of unbroken generators. In the case of $SU(4) \times SU(2) \times SU(2)$, the unbroken group has dimension:

$$\dim[SU(4)] + \dim[SU(2)] + \dim[SU(2)] = 15 + 3 + 3 = 21 \quad (3.28)$$

So there should remain 21 unbroken generators, which is correct for the VEV we defined. To determine which generators remain unbroken, we use the commutator test. For a VEV ϕ transforming under an $SO(10)$ representation, its infinitesimal transformation under the Lie algebra generator T_a is given by

$$\delta\phi = i[T_a, \phi], \quad (3.29)$$

when dealing with matrix-valued representation like the **45** and **54**. Similarly for vector representation:

$$\delta\phi = iT_a\phi. \quad (3.30)$$

A generator T_a is unbroken under the VEV if and only if the VEV is invariant under its action:

$$[T_a, \phi] = 0. \quad (3.31)$$

Any group element of a continuous group can be written as an exponential of generators:

$$g = e^{i\alpha^a T_a} = 1 + i\alpha^a T_a + \frac{1}{2}(i\alpha^a T_a)(i\alpha^b T_b) + \dots \quad (3.32)$$

The condition that the VEV is invariant under the full group element, $g\langle\phi\rangle = \langle\phi\rangle$, becomes:

$$\left(1 + i\alpha^a T_a + \frac{1}{2}(i\alpha^a T_a)(i\alpha^b T_b) + \dots\right) \langle\phi\rangle = \langle\phi\rangle. \quad (3.33)$$

Solving order-by-order:

- **First order** ($\mathcal{O}(\alpha)$): $T_a \langle\phi\rangle = 0$ for all unbroken generators.
- **Second order** ($\mathcal{O}(\alpha^2)$): $T_a T_b \langle\phi\rangle = 0$ for all unbroken generators.

We can decompose the second-order term using:

$$T_a T_b = \frac{1}{2} (\{T_a, T_b\} + [T_a, T_b]), \quad (3.34)$$

where $[T_a, T_b] = i f_{abc} T_c$ by the Lie algebra structure. This commutator gives another generator that can be satisfied by the first-order condition. So, for the second-order equation, to see which generators are unbroken besides the first-order solutions, we need to solve the anti-commutator: $\{T_a, T_b\}$. Together, these two highest orders give all unbroken generators. Higher orders are automatically satisfied by these two highest orders.

To make sure the unbroken generators that are found in this process do form the right subgroup, it is important to check that the amount of unbroken generators equals the dimension of the subgroup of interest, and that the commutation of the found unbroken generators give linear equations of unbroken generators only. This is to verify that the unbroken generators form a closed algebra.

This process can then be repeated for all other subgroups. The Mathematica code in this thesis was made with the help of the large language models Claude by Anthropic [4] and ChatGPT by OpenAi [30]. These were used for debugging, syntax optimisation and implementation suggestions. All mathematical derivations, physical interpretations and final code validation were performed independently.

So, to summarise the taken steps:

- 1. Construct the generator matrices of $SO(10)$ in the relevant representation.
- 2. Define a candidate VEV based on the characteristics of the representation.
- 3. Compute the commutators with all the generators.
- 4. Count the number of generators that annihilate the VEV and make sure the subgroup of interest matches the dimension.

The amount of unbroken generators can simply be found by counting the dimensions of the relevant subgroup(s). These can be found in table 3.3.

Subgroup	Unbroken generators
$SO(9)$	36
$SO(8) \times U(1)$	29
$SO(7) \times SU(2)$	24
$SU(5) \times U(1)$	25
$Sp(4) \times Sp(4)$	20
$SU(4) \times SU(2) \times SU(2)$	21
$Sp(4)$	10

Table 3.3: Amount of unbroken generators per subgroup of $SO(10)$.

This way, the VEVs of the subgroups of $SO(10)$, and other groups, can be determined.

The last subgroup that we have not yet discussed is $Sp(4)$. This group obtains a singlet for the 120-representation; $120 = 1 + 5 + 14 + 30 + 35 + 35'$. For this case, very little literature is found, so a different method was implemented. In [38], the following projection matrix was found:

$$P = \begin{pmatrix} 2, 2, 4, 1, 1 \\ 0, 1, 0, 1, 1 \end{pmatrix} \quad (3.35)$$

With the LieArt function `WeightSystem[Irrep [SO10][120]]` we find the full weight system of the **120** representation of $\mathfrak{so}(10)$. These weights are then multiplied with the projection matrix to find the weights of the **120** representation of $\mathfrak{Sp}(4)$. The next step was to identify the $Sp(4)$ -singlet directions, so the weights that project to the zero vector under the projection matrix.

This then yields 8 weights that project to a $(0, 0)$. This does not suggest eight different singlets, these eight $SO(10)$ weights project to the same $Sp(4)$ weight. These eight weights all span a one-dimensional subspace, as they are linearly dependent, meaning that there is only one independent singlet direction.

Now, to finally construct the VEV, we assign a free parameter v to each independent singlet direction. This means that our VEV has 8 nonzero components. This way we obtained the VEV as can be seen in table 3.2. This method is not as straightforward as the one we used earlier, but it allows us to systematically check all candidate VEVs, ensuring that the correct unbroken subgroup is preserved, even when the representation is large and nontrivial, such as 120.

3.3.2 Connection to other research

In this chapter we have found the methods that allow us to systematically determine the VEVs that correspond to the symmetry-breaking patterns of $SO(10)$. While this analysis seems mathematical, it is very relevant to physical applications: by identifying all possible subalgebras and their corresponding VEVs, we can determine which symmetry-breaking chain corresponds to the global minimum of the scalar potential. The framework developed here provides the foundation for systematic studies of $SO(10)$ breaking patterns. Held et al. [23] pioneered a method to compare different breaking chains by evaluating their vacuum energies, which was subsequently implemented numerically by Magnus Petz [32]. Petz performed large-scale numerical scans of the $SO(10)$ scalar potential parameter space for a specific model with VEVs in the **16** (spinor) and **45** (adjoint) representations. His analysis demonstrated that:

- The residual symmetry is parameter-dependent. He found that different coupling constants in the scalar potential lead to different symmetry breaking patterns. The regions of parameter space that break to the SM are only part of the full parameter space. Choosing different parameters, leads to different symmetries. This is visualised in Figure 3.1, which is an analogue of figure 7.2 in [32]. These plots show on the axes the parameters used (λ_i) and with colours the breaking results. The green areas show the parameter space where there is an allowed VEV texture, so there is a viable breaking pattern. Red on the other hand shows where there the VEV texture is not allowed and thus where there is no viable breaking. In Figure 3.2, analogue of figure 7.4 of [32], we see where specific cases of the VEV texture lead to breaking and to which symmetry it breaks to for those parameters. Here, the Standard Model is only a part of this parameter space.
- The breaking scale varies. Even in the regions where $SO(10)$ breaks to the Standard Model, the energy scale at which this breaking occurs varies. For some parameters this breaking occurs at 10^{10}GeV , but for others it could be near the Planck scale at 10^{16}GeV . This matters in this research as well as this is an experimental constraint on which scales are allowed based on Higgs mass, top quark mass, and other qualities.

So, while our research gives the framework on the possible subgroups and VEVs of $SO(10)$, Petz's work shows (for a specific case) which of those VEVs really minimises the energy for different parameters. These works together give future researchers the complete picture on what symmetry breaking chain will give the true energy minimum.

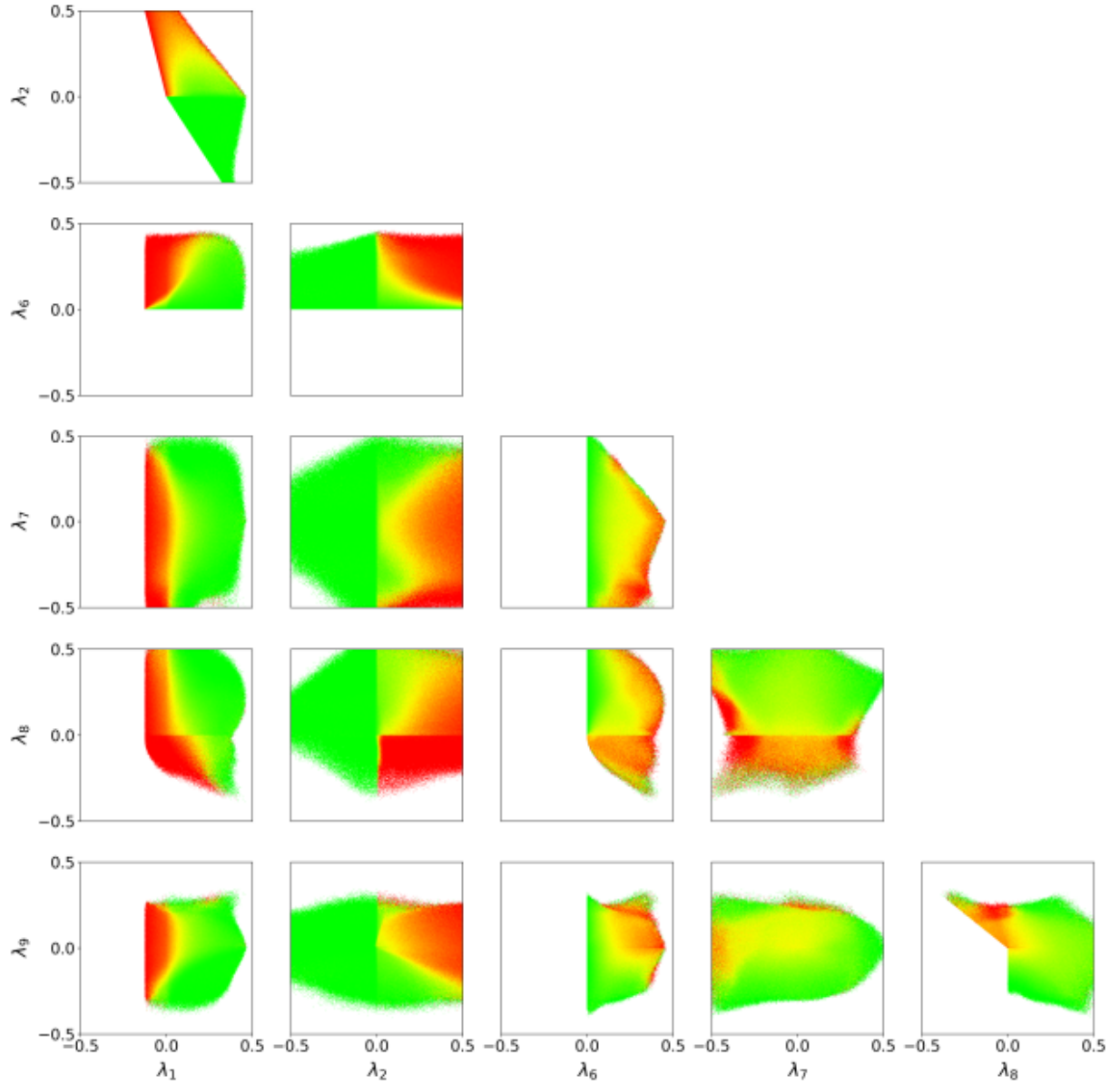


Figure 3.1: Parameter scan for $SO(10)$ symmetry breaking, from [32]. The axes represent coupling constants λ_i in the scalar potential for an $SO(10)$ model with $16_H \oplus 45_H$ scalars. Green regions indicate parameter combinations where viable VEV textures exist. Red regions correspond to unphysical/unstable configurations.

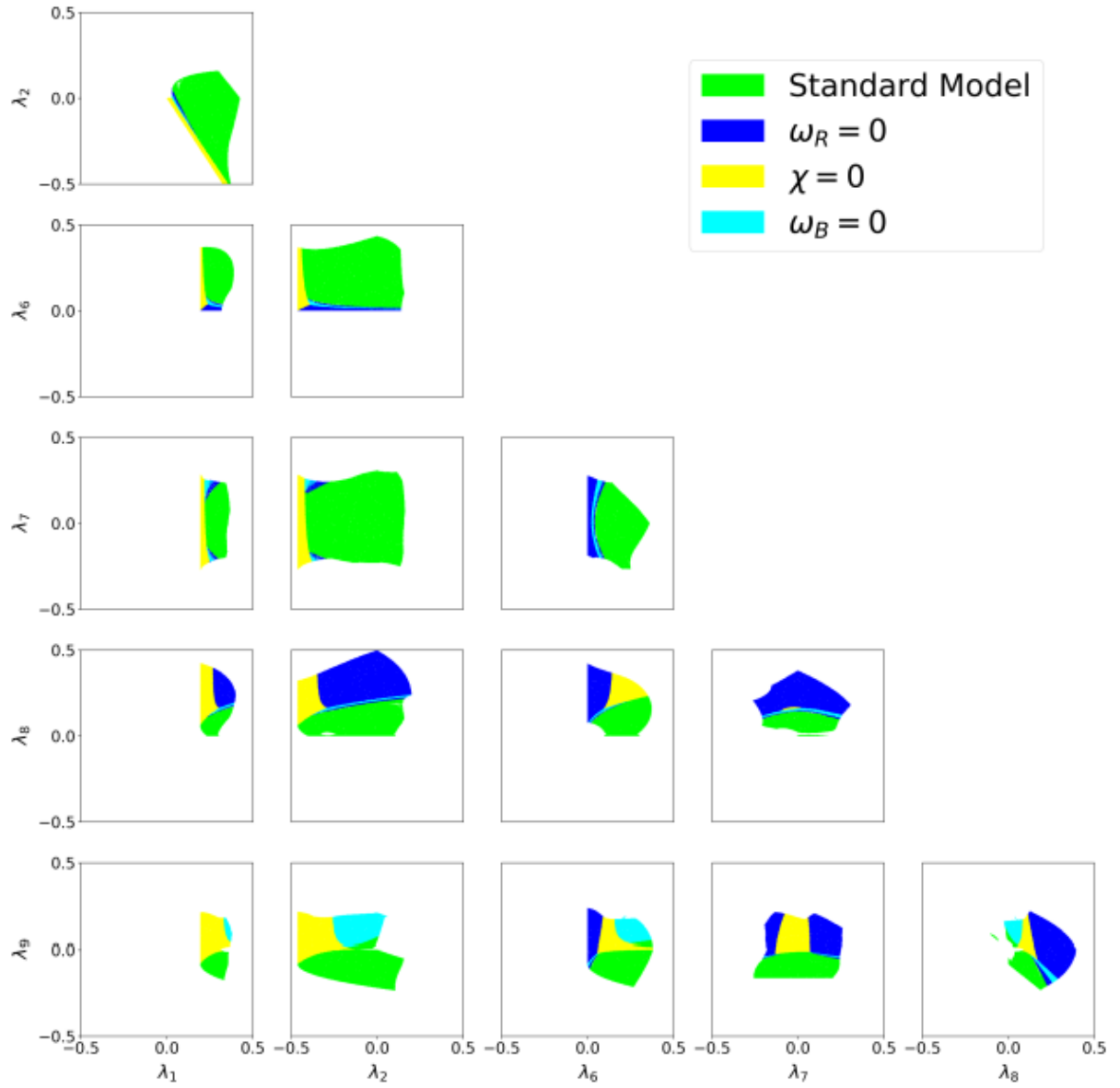


Figure 3.2: Specific VEV texture parameter regions, from [32]. A detailed parameter space scan showing regions where specific VEV configurations lead to particular breaking patterns. The colour coding identifies which residual symmetry groups survive for different coupling constant combinations.

Now that we have established systematic methods for determining VEVs that break $SO(10)$ to its maximal continuous subgroups, we turn to a different question: can continuous symmetries break to discrete residual subgroups? In the next chapter, we investigate how VEVs in representations of the continuous group $SU(3)$ can break the symmetry down to the discrete group A_4 , leaving no continuous symmetry unbroken.

Chapter 4

Residual discrete symmetries from $SU(3)$

Having seen how VEVs work for continuous groups, it is now time to expand our knowledge to discrete groups. For this thesis we will look into the breaking $SU(3) \rightarrow A_4$ specifically. The reason for this is up until now we have only discussed the local symmetry $SO(10)$. While $SO(10)$ unifies gauge interactions, it does not explain the origin of flavour structure. The observed fermion masses span a great range, from about 10^{-2} eV for neutrinos, to about 173GeV for the top quark. In the same way, the quark mixing angles are small relative to the large neutrino mixing angles. To understand these hierarchies, we need an additional ingredient: a global symmetry acting on the three fermion generations.

Such a group must have a triplet representation, to unify the three families. It needs to act unitarily, so we can write kinematic terms, and it needs to be connected and continuous at high energies to match the expectation that near the Planck scale all symmetries are restored. The minimal choice that satisfies these requirements is $SU(3)_{\text{global}}$. When this global symmetry breaks via VEV textures, the breaking pattern determines fermion mass matrix structures, naturally generating the hierarchies we observe. The breaking also produces Goldstone bosons contributing to the effective theory at lower energies. When breaking to a finite group, as we will do in this chapter, these Goldstone bosons acquire a small mass. These Goldstone bosons are actually called pseudo-Goldstone bosons, or pNG bosons. For the present analysis however, we focus mostly on the residual symmetry structure rather than the detailed Goldstone phenomenology.

The continuous group $SU(3)$ cannot survive unbroken at low energies, since this would predict equal masses for all three generations. Instead, it must break to a discrete residual symmetry. Neutrino oscillation experiments reveal large mixing angles for leptons, compared to quark mixing, suggesting a discrete flavour symmetry. The minimal group with a three-dimensional irreducible representation capable of producing such mixing patterns is A_4 . A_4 was originally put forth as an ideal symmetry for this issue as it explained the mathematical structure of the tri-bimaximal mixing (TBM) matrix very well [1].

4.1 A_4 leading to Tri-bimaximal Mixing

In 2005, it was proposed by Altarelli and Feruglio in [1] that the A_4 symmetry group leads to TBM. The tri-bimaximal mixing we refer to here is the specific pattern that the neutrino mixing matrix seems to have:

$$|U_{\text{PMNS}}| = \begin{pmatrix} \sqrt{2/3} & \sqrt{1/3} & 0 \\ \sqrt{1/6} & \sqrt{1/3} & \sqrt{1/2} \\ \sqrt{1/6} & \sqrt{1/3} & \sqrt{1/2} \end{pmatrix}. \quad (4.1)$$

To show this, they assign leptons to the four representations of A_4 . The left handed lepton doublets transform as a triplet **3**. The right-handed charged leptons transform as the singlet representations. The scalar fields take the form $\phi = (\phi_1, \phi_2, \phi_3) \sim \mathbf{3}$ and $\xi \sim \mathbf{1}$, assigned to the A_4 triplet and singlet respectively. These fields acquire the VEVs: $\langle \phi \rangle = (v, v, v)$ and $\langle \xi \rangle = u$. The neutrino mass matrix that is obtained from these VEV is then of the form:

$$\begin{pmatrix} 2A + B & -A & -A \\ -A & 2A & B - A \\ -A & B - A & 2A \end{pmatrix}. \quad (4.2)$$

This mass matrix leads to exact tri-bimaximal mixing in this model. The intricacies of this Altarelli-Feruglio model are very well discussed in [15] by Wouter Dekens. This model is based on [1] and [2] by Alterelli and Feruglio. This model was very promising and did seem to clearly indicate that A_4 is a good choice as a residual symmetry after breaking $SU(3)$ flavour, since it leads to the exact neutrino mixing we saw in experiments, namely the mixing angles $\theta_{12} = 35^\circ$, $\theta_{23} = 45^\circ$, $\theta_{13} = 0^\circ$. The prediction of these mixing angles has however been falsified experimentally. It was found that the angle $\theta_{13} = 8.5^\circ$ and not zero [29], [3]. However, A_4 is still a group of interest as it is still able to describe the current mixing matrices with deviations [33, 28]. This is why it is important to understand the breaking of $SU(3)$ to A_4 , as it could be able to complete our GUT theory.

4.2 $SU(3) \rightarrow A_4$

A_4 , or $\Delta(12)$, is a tetrahedral group. The group contains the even permutations of four objects, meaning it consists of 12 elements. A_4 has a presentation with two generators a, b , as:

$$A_4 : a^2 = b^3 = (ab)^3 = e \quad (4.3)$$

As mentioned in the introduction, we are interested in A_4 as a subgroup of $SU(3)$. To understand this breaking we first need to know for which representations the breaking of $SU(3)$ gives a singlet state of A_4 .

As can be seen in table 4.2, the smallest representations for which the A_4 obtains a singlet are **6**, **10** and **15**, meaning that these representations can be used to break $SU(3)$ to A_4 , or a group that has A_4 as a subgroup. Our goal here is to find the VEV for the lowest representation that breaks $SU(3)$ to A_4 , where A_4 is the maximal unbroken symmetry, meaning that there are no larger symmetries that remain after breaking $SU(3)$. In [26], it was found that the combination of the VEV of the **6** and **10** representations breaks $SU(3)$ down to A_4 as a maximal subgroup. To test this ourselves we have used the code that is explained here.

$SU(3)$ rep.	A_4 decomposition
3	3
6	1 + 1' + $\bar{1}' + 3$
8	$1' + \bar{1}' + 2 \cdot 3$
10	$1 + 3 \cdot 3$
15	$1 + 1' + \bar{1}' + 4 \cdot 3$

Table 4.1: Branching rules of $SU(3) \supset A_4$ [27].

In this code, we have defined the generators of $\mathfrak{su}(3)$ in the **6** representation and in the **10** representation. These are defined using the Gell-Mann matrices: $F_i = \frac{\lambda_i}{2}$. Here, first the six dimensional representation was constructed using the tensor product of $SU(3)$: $3 \otimes 3 = 6 \oplus \bar{3}$. This means that the **6** representation corresponds to the symmetric product of the two triplets.

Listing 4.1: Constructing the 6-dimensional $SU(3)$ matrices.

```
MakeSixRep[T3x3_] := Module[{T6},
  T6 = Table[0, {6}, {6}];
  T6[[1, 1]] = 2*T3x3[[1, 1]]; T6[[1, 4]] = Sqrt[2]*T3x3[[1, 2]]; T6
  [[1, 6]] = Sqrt[2]*T3x3[[1, 3]];
  T6[[2, 2]] = 2*T3x3[[2, 2]]; T6[[2, 4]] = Sqrt[2]*T3x3[[2, 1]]; T6
  [[2, 5]] = Sqrt[2]*T3x3[[2, 3]];
  T6[[3, 3]] = 2*T3x3[[3, 3]]; T6[[3, 5]] = Sqrt[2]*T3x3[[3, 2]]; T6
  [[3, 6]] = Sqrt[2]*T3x3[[3, 1]];
  T6[[4, 1]] = Sqrt[2]*T3x3[[2, 1]]; T6[[4, 2]] = Sqrt[2]*T3x3[[1,
  2]];
  T6[[4, 4]] = T3x3[[1, 1]] + T3x3[[2, 2]]; T6[[4, 5]] = T3x3[[1,
  3]]; T6[[4, 6]] = T3x3[[2, 3]];
  T6[[5, 2]] = Sqrt[2]*T3x3[[3, 2]]; T6[[5, 3]] = Sqrt[2]*T3x3[[2,
  3]];
  T6[[5, 4]] = T3x3[[3, 1]]; T6[[5, 5]] = T3x3[[2, 2]] + T3x3[[3,
  3]]; T6[[5, 6]] = T3x3[[2, 1]];
  T6[[6, 1]] = Sqrt[2]*T3x3[[3, 1]]; T6[[6, 3]] = Sqrt[2]*T3x3[[1,
  3]];
  T6[[6, 4]] = T3x3[[3, 2]]; T6[[6, 5]] = T3x3[[1, 2]]; T6[[6, 6]] =
  T3x3[[1, 1]] + T3x3[[3, 3]];
  Return[T6];
];
```

Using these generators, the VEV that was found in [26] $\phi = \{1, 1, 1, 0, 0, 0\}$ was multiplied with all the generators to find the generators and linear combination of generators that left the VEV invariant. It was found that the second, fifth and seventh generator, or equivalently, λ_2 , λ_5 and λ_7 , leave the VEV invariant. These three generators form the Lie algebra of $\mathfrak{so}(3)$. So, this VEV breaks $\mathfrak{su}(3)$ to $\mathfrak{so}(3)$.

Next, we see whether the VEV of the **10** indeed breaks $\mathfrak{so}(3)$ to A_4 . For this we need the generators of the **10** representation. The **10** of $SU(3)$ is the completely symmetric part of $3 \otimes 3 \otimes 3$, so we start again with the generators of the **3**, $F_i = \frac{\lambda_i}{2}$. For each generator F_i , the action on the triple

tensor product is:

$$F_i^{(27)} = F_i \otimes I \otimes I + I \otimes F_i \otimes I + I \otimes I \otimes F_i, \quad (4.4)$$

giving an explicit 27×27 matrix.

Listing 4.2: Construction of 27-dimensional $3 \otimes 3 \otimes 3$ representation.

```
MakeTensor27[T3x3_] := Module[{I3, T27},
  I3 = IdentityMatrix[3];
  T27 = KroneckerProduct[T3x3, I3, I3] +
    KroneckerProduct[I3, T3x3, I3] +
    KroneckerProduct[I3, I3, T3x3];
  Return[T27];
];
```

Now, we need to build an orthonormal basis of symmetrised states, covering all ten symmetric combinations.

Listing 4.3: Construction of the symmetric projection operator.

```
(* Function to convert (i,j,k) -> flat index, \
where mathematica indexes from 1*)
FlatIndex[i_, j_, k_] := (i - 1) + 3*(j - 1) + 9*(k - 1) + 1;

(* list all (i,j,k) combinations *)
allTriples =
  Flatten[Table[{i, j, k}, {i, 1, 3}, {j, 1, 3}, {k, 1, 3}], 2];

symBasis = {
  {{1, 1, 1}}, (* 1 permutations *)
  {{2, 2, 2}}, (* 1 permutations *)
  {{3, 3, 3}}, (* 1 permutations *)
  {{1, 1, 2}, {1, 2, 1}, {2, 1, 1}}, (* 3 permutations *)
  {{1, 1, 3}, {1, 3, 1}, {3, 1, 1}}, (* 3 permutations *)
  {{1, 2, 2}, {2, 1, 2}, {2, 2, 1}}, (* 3 permutations *)
  {{2, 2, 3}, {2, 3, 2}, {3, 2, 2}}, (* 3 permutations *)
  {{1, 3, 3}, {3, 1, 3}, {3, 3, 1}}, (* 3 permutations *)
  {{2, 3, 3}, {3, 2, 3}, {3, 3, 2}}, (* 3 permutations *)
  {{1, 2, 3}, {1, 3, 2}, {2, 1, 3}, {2, 3, 1}, {3, 1, 2}, {3, 2, 1}} (* 6 permutations *)
};

(* Normalised basis vectors in 27-dim space *)
symBasisVectors = Table[
  Module[{vec, perms, norm},
    vec = Table[0, {27}];
    perms = symBasis[[i]];
    norm = Sqrt[Length[perms]];
    Do[
      vec[[FlatIndex @@ perm]] = 1/norm,
      {perm, perms}
    ];
    vec
  ],
  {i, 1, 10}
];
```

```

    {perm, perms}
];
vec
],
{i, 1, 10}
];

```

Then to find the 10-dimensional generators, we project the 27-dimensional matrices onto the defined symmetric tensors by;

$$T_{ij}^{(10)} = \langle e_i | T^{(27)} | e_j \rangle \quad (4.5)$$

Listing 4.4: Project 27-dimensional generators on 10-dimensional subspace.

```

F10 = Table[
  Table[
    symBasisVectors[[i]] . F27[[gen]] . symBasisVectors[[j]],
    {i, 1, 10}, {j, 1, 10}
  ],
  {gen, 1, 8}
];

```

This method then yields us eight Hermitian 10×10 matrices that satisfy the $SU(3)$ algebra.

Now, that we have obtained the explicit matrices of the **10** of $SU(3)$, we can apply the VEV found in [26]: $\phi = \{0, 0, 0, 0, 0, 0, 0, 0, 0, 0, 1\}$. We apply this VEV to the generators that remain unbroken after applying the VEV of the **6**, so the **10** generators corresponding to λ_2, λ_5 and λ_7 . This action yields the following:

$$\lambda_2 \cdot \{0, 0, 0, 0, 0, 0, 0, 0, 0, 0, 1\} = \{0, 0, 0, 0, -\frac{i}{\sqrt{2}}, 0, \frac{i}{\sqrt{2}}, 0, 0, 0\}, \quad (4.6)$$

$$\lambda_5 \cdot \{0, 0, 0, 0, 0, 0, 0, 0, 0, 0, 1\} = \{0, 0, 0, -\frac{i}{\sqrt{2}}, 0, 0, 0, 0, \frac{i}{\sqrt{2}}, 0\}, \quad (4.7)$$

$$\lambda_7 \cdot \{0, 0, 0, 0, 0, 0, 0, 0, 0, 0, 1\} = \{0, 0, 0, 0, 0, -\frac{i}{\sqrt{2}}, 0, \frac{i}{\sqrt{2}}, 0, 0\}. \quad (4.8)$$

This means that all of the unbroken generators that were left after applying the **6** VEV are broken after applying the **10** VEV, and that the continuous symmetry is completely broken. Now, there can only be a discrete symmetry leftover, or no symmetry at all.

To see whether a discrete subgroup survives, we multiply all the generators of the discrete subgroups of $SU(3)$ with the two VEVs. The finite subgroups and their generators can be found in table 4.2.

The explicit group generators matrices of these finite groups can be found in chapter6 and are from [22]. These matrices are all 3-dimensional, meaning that we still need to make them 6- and 10-dimensional to apply the VEVs. For this, we use the same method as before for the $SU(3)$ matrices.

When multiplying the group generators with the **6** VEV, only $A(2), B, E, W$, and Z survive. These correspond to the groups; $\Sigma(60)$, $\Delta(12)$, and $\Delta(24)$, meaning that these finite groups survive the **6** VEV.

Subgroup	Order	Generators
$\Sigma(60)$	60	A, E, W
$\Sigma(168)$	168	Y, E, Z
$\Sigma(36 \times 3)$	108	C, E, V
$\Sigma(72 \times 3)$	216	C, E, V, X
$\Sigma(216 \times 3)$	648	C, E, V, D
$\Sigma(360 \times 3)$	1080	A, E, W, F
$\Delta(3n^2)(n \geq 2)$	$3n^2$	$A(n), E$
$\Delta(6n^2)(n \geq 1)$	$6n^2$	$A(n), E, B$

Table 4.2: The finite subgroups of $SU(3)$ with their respective generators. From [22].

Subgroup	6-VEV	10-VEV
$\Sigma(60)$	$\Sigma(60)$	\times
$\Sigma(168)$	\times	\times
$\Sigma(36 \times 3)$	\times	\times
$\Sigma(72 \times 3)$	\times	\times
$\Sigma(216 \times 3)$	\times	\times
$\Sigma(360 \times 3)$	\times	\times
$\Delta(3n^2)(n \geq 2)$	$\Delta(12)$	$\Delta(3n^2)(n \geq 2)$
$\Delta(6n^2)(n \geq 1)$	$\Delta(24)$	\times

Table 4.3: The finite subgroups of $SU(3)$ and which survive the respective VEVs $\{1, 1, 1, 0, 0, 0\}$ and $\{0, 0, 0, 0, 0, 0, 0, 0, 0, 1\}$. An \times means that the generators of that subgroup do not survive the VEV of interest.

After multiplying the group generators with the **10** VEV, only $A(n), D, E$, and Y survive. These correspond to the $\Delta(3n^2)$ groups for $n \geq 2$. This means that only these groups survive the **10** VEV. This is shown in table 4.3.

Combining these results, we find that only $\Delta(12)$, or A_4 as these are the same, survives both VEVs. This means that the combination of the **6** VEV $\phi = \{1, 1, 1, 0, 0, 0\}$ and the **10** VEV $\{0, 0, 0, 0, 0, 0, 0, 0, 0, 1\}$ gives rise to an A_4 symmetry, and no larger symmetry.

Since the **6** VEV breaks $SU(3) \rightarrow SO(3)$, we should understand which discrete subgroups $SO(3)$ possesses. The complete classification is given in table 4.4. Importantly, $A_4 \cong T$ (both have order 12), so the residual A_4 symmetry corresponds to tetrahedral symmetry.

4.3 Different order of VEVs

Up until now we have only looked at applying the **6** VEV and then the **10** VEV to the $SU(3)$ group generators. However, what happens when we switch the order, so when we apply the **10** VEV first? When multiplying the VEV $\{0, 0, 0, 0, 0, 0, 0, 0, 0, 1\}$ with the 10-dimensional $SU(3)$ generators, we find that only the generators corresponding to λ_3 and λ_8 survive. These generators form the Lie algebra of $\mathfrak{u}(1) \times \mathfrak{u}(1)$. From multiplying the generators of the finite subgroup of $SU(3)$ with the **10** VEV, we know that the finite group $\Delta(3n^2)$ also survives. This is not a subgroup of $U(1)$, so needs

Finite subgroup	Description	Order	Generators
C_k	Cyclic	k	R
D_k	Dihedral	$2k$	x, y
T	Tetrahedral	12	T_1, T_2
O	Octahedral	24	O_1, O_2, O_3
I	Icosahedral	60	I_1, I_2, I_3

Table 4.4: Finite subgroups of $SO(3)$, from [12], [5], [6], [14]. The matrix generators can be found in the appendix, chapter 6.

to be coupled to the continuous symmetry. This means that the complete surviving symmetry after applying the **10** VEV is $U(1) \times U(1) \times \Delta(3n^2)$ for $n \geq 2$. We will now apply the **6** VEV and see for what α_i the generators survive:

$$e^{i\alpha_3\lambda_3} \cdot e^{i\alpha_8\lambda_8} \cdot \{0, 0, 0, 0, 0, 0, 0, 0, 0, 1\} = \{0, 0, 0, 0, 0, 0, 0, 0, 0, 1\} \quad (4.9)$$

This is only the case for $\alpha_3 = \pi(n - m)$ and $\alpha_8 = \sqrt{3}\pi(n + m)$, where $n, m \in \mathbb{Z}$. This means that the continuous symmetry is broken, as there is only a discrete set of solutions, not a continuous curve or region. With this we get the following group elements:

$$U_1 = 1 \quad U_2 = e^{i\pi\lambda_3} e^{i\pi\lambda_8} \quad U_3 = e^{i2\pi\lambda_3} \quad U_4 = e^{i2\pi\sqrt{3}\lambda_8}$$

So, we find a group of order 4. This can only be \mathbb{Z}_4 or $\mathbb{Z}_2 \times \mathbb{Z}_2$. Since our U_i 's are commutative and non-cyclic, we are dealing with $\mathbb{Z}_2 \times \mathbb{Z}_2$, also called the Klein four group. From breaking the generators of the finite subgroups of $SU(3)$ we know that the A_4 finite group must also survive the VEV breaking of both VEVs. The remaining question here is then, is the found Klein four group part of A_4 or is it a separate discrete symmetry? To investigate this, Mathematica was again used to see whether the explicit generators of the Klein four group that we found after applying the **6** VEV, are the same as the generators of the A_4 group. When comparing these generators, we do indeed find they are the same. Specifically, the found Klein four group consists of the identity plus three elements of the order 2, which are precisely the generators we had for A_4 . The fact that our Klein four group form λ_3 and λ_8 matches part of the generators of A_4 means that this is not an independent symmetry but rather a natural subgroup that is already contained in A_4 .

Therefore, the final residual symmetry after applying both VEVs is:

$$SU(3) \xrightarrow{10\text{-VEV}} U(1) \times U(1) \times \Delta(3n^2) \xrightarrow{6\text{-VEV}} A_4 \quad (4.10)$$

While we do end up with our A_4 symmetry again, as we wanted, the order does make a difference in the resulting symmetry. With the **6** VEV first, we had the continuous symmetry $SO(3)$ left, but with the **10** VEV first we found $U(1) \times U(1) \times \Delta(3n^2)$. This means that the ordering of the VEV makes a difference in what symmetry we find. This is interesting as in most sources, like [26] where we found our VEVs, there is no notion of a certain order the VEVs should be applied.

Now, to summarise, a schematic of the breaking of $SU(3)$ can be seen in figure 4.1. Here, the amount of Goldstone and pseudo-Goldstone bosons are added. As can be seen, the total amount of bosons for both breaking chains is equal to 8, as $SU(3)$ has 8 generators.

After applying the **6** VEV first, three generators survive, λ_2, λ_5 and λ_7 . These three generate $SO(3)$ but also the discrete group A_4 . This can be seen explicitly when we exponentiate the generators of A_4 in the **3** representation. In matrix form, these are:

$$S = \begin{pmatrix} 1 & 0 & 0 \\ 0 & -1 & 0 \\ 0 & 0 & -1 \end{pmatrix}, T = \begin{pmatrix} 0 & 1 & 0 \\ 0 & 0 & 1 \\ 1 & 0 & 0 \end{pmatrix}. \quad (4.11)$$

When exponentiating these matrices, we find that these give the following values:

$$S = e^{i\pi\lambda_7}, T = e^{\frac{2\pi i}{3\sqrt{3}}(\lambda_2 - \lambda_5 + \lambda_7)} \quad (4.12)$$

This shows that the generators of the **3** representation of A_4 can indeed be made out of the unbroken generators λ_2, λ_5 and λ_7 .

Now, since we found that three generators survive, while the other five break to $SO(3)$, we must have five Goldstone bosons. When we now break these three generators further, using the **10** VEV, we find that the continuous group breaks to a discrete group, A_4 . To generate A_4 we need two generators. This means that we have only one completely broken generator, which becomes a massless Goldstone boson and two generator combinations that still generate the discrete symmetry A_4 and become pseudo-Goldstone bosons. These two get mass because the continuous symmetry is not entirely broken. There is still a discrete symmetry left.

For the other path, we apply the **10** VEV first. Two generators are necessary to produce $\Delta(3n^2)$. Since we break a continuous symmetry to a discrete one, this means we obtain two pseudo-Goldstone bosons. Two continuous generators survive for $U(1) \times U(1)$. These are λ_3 and λ_8 as we saw before. This means that we obtain four Goldstone bosons too, since $8 - 2 - 2 = 4$. Then, when we apply the second VEV, the **6**, we are only left with a discrete group, meaning that our remaining continuous generators must be broken completely, giving us two Goldstone bosons. This explains figure 4.1 and the Goldstone bosons in our theory.

In this chapter, we have found that A_4 is indeed a subgroup of $SO(3)$. To prove this we have used the 6-dimensional VEV $\{1, 1, 1, 0, 0, 0\}$ and the 10-dimensional VEV $\{0, 0, 0, 0, 0, 0, 0, 0, 0, 1\}$. According to [26] these are the lowest dimensional VEVs that break $SU(3)$ exclusively to A_4 . This is indeed the case, no matter the order we apply the VEVs. We did find however that when we switch the order, we obtain a different intermediate symmetry, $SO(3)$ vs. $U(1) \times U(1) \times \Delta(3n^2)$. This is not expected and is an interesting result, as the importance of order is not mentioned in existing literature.

Most works, such as [26], present VEV configurations without specifying any sequence, or preferred order. They implicitly assume order-independence. Our explicit calculation shows this assumption is incorrect: the intermediate symmetry depends crucially on VEV ordering. As we have also seen in figure 4.1, the distribution of Goldstone bosons also differs between breaking stages. Again, a feature that affect physics at low energies.

Now that we have this final result, we move on to discuss all our findings and their consequences.

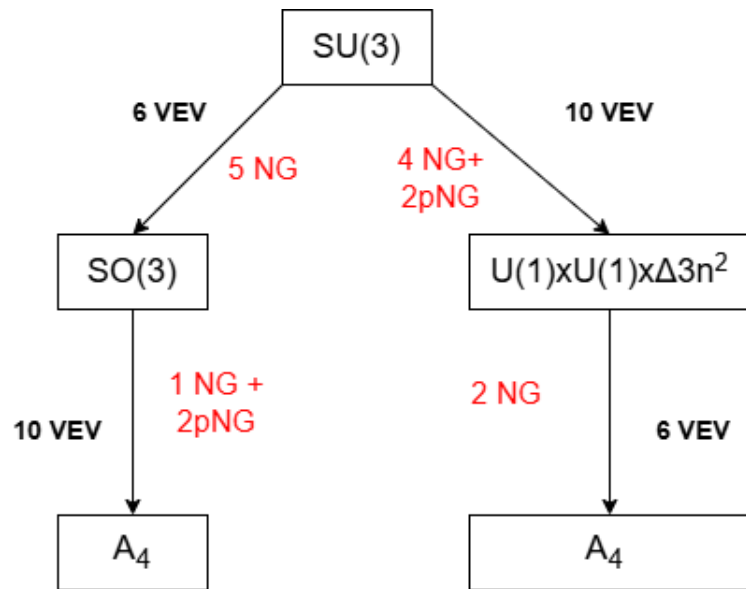


Figure 4.1: Schematic breaking of $SU(3)$, using both VEV orderings. The amount of Nambu Goldstone bosons (NG) and pseudo-Nambu Goldstone bosons (pNG) we obtain with each breaking are listed in red.

Chapter 5

Conclusion

This thesis developed a systematic framework for understanding symmetry breaking in Grand Unified Theories and flavour physics. We addressed two main questions: what breaking patterns exist for $SO(10)$ beyond the standard route to the SM, and how can discrete flavour symmetries like A_4 emerge from continuous group breaking?

5.1 Main Results

5.1.1 $SO(10)$ Breaking Patterns

In the first part of our research, we classified all maximal subalgebras of $SO(10)$ and determined the minimal VEV configurations for each breaking pattern. The literature typically assumes $SO(10) \rightarrow SU(5) \rightarrow SM$, but this is only one of many mathematically allowed routes. Alternative routes are equally valid according to group theory.

The key point is that the actual breaking pattern depends on which configuration minimises the scalar potential. We cannot assume the SM corresponds to the true energetic minimum without explicit calculations. Crucially, the approach of finding the absolute minimum, as developed by Held et al. in [23] and extended by Magnus Petz in [32], can only be complete if one can check all possible minima. This in turn requires a complete classification of all breaking chains and VEVs that can exist. The systematic classification in this thesis provides exactly this. By identifying all the maximal subgroups and their VEV configurations, we establish the complete set of possible breaking patterns that must be compared energetically. This enables the approach of Held and Petz to be fully implemented, such that future work can now compute the potential depth for each classified texture.

For our framework in this thesis, we first identified each maximal subgroup. For each of these, we identified the minimal scalar representation containing a singlet and constructed explicit VEV textures. Using Mathematica, we developed methods for building the generators of the relevant representations and systematically checked which generators remain unbroken. This method can be implemented for all subgroups, not just the maximal ones we focused on in this research.

5.1.2 $SU(3) \rightarrow A_4$ breaking

Beyond gauge unification, we also investigated discrete flavour symmetries emerging from $SU(3)_{global}$. The fermion mass hierarchies and the contrast between the small quark mixing angle and large lepton mixing angle are not explained by only a local symmetry. The global symmetry $SU(3)$ provides a framework for generating these structures through breaking patterns. At high energies, $SU(3)$ treats the three fermion generations as a triplet. By breaking the continuous symmetry at lower scales, it produces hierarchical mass matrices. At low energies, the continuous symmetry should be broken, as it would otherwise predict equal masses for all generations. Instead, a discrete residual symmetry must remain.

In this thesis, we focused on A_4 , the minimal non-abelian group with a three-dimensional irrep, which reproduces large neutrino mixing angles. Using VEVs in the 6-dimensional representation $\{1, 1, 1, 0, 0, 0\}$ and 10-dimensional representation $\{0, 0, 0, 0, 0, 0, 0, 0, 0, 1\}$, we showed explicitly how $SU(3)$ breaks to A_4 .

5.1.3 Order dependence

The most surprising result of this thesis is that the order of VEV application matters. Applying both VEVs indeed gives the discrete group A_4 as the maximal residual symmetry. However, reversing the order produces a different intermediate symmetry, $SO(3)$ for first the **6** VEV and $U(1) \times U(1) \times \Delta(3n^2)$ for first the **10** VEV. This is not widely discussed in literature, where multiple VEVs are used without specifying their order.

This means future researchers must carefully specify not just which VEVs break symmetries, but also their hierarchy and the resulting intermediate symmetries.

5.2 Future Research

This research still leaves a lot of questions for future research.

First of all, is the question which $SO(10)$ breaking pattern has the lowest energy minimum. This question can now be answered by combining the VEV and subalgebra framework provided in this work with the numerical methods provided by Petz in [32]. Then, they can answer whether $SO(10) \rightarrow SU(5) \rightarrow SM$ indeed has the lowest energy minimum for some region in parameter space, of all the other breaking patterns. This could strengthen our current work on the Standard Model if this path indeed has the energy minimum, but it could also mean that we need to rethink our GUT theories.

Secondly, we need to find a way to couple $SO(10)_{local}$ and $SU(3)_{local}$. In this research we treated the gauge and flavour symmetries independently, but to create the complete GUT theory we have talked about, there needs to be a way to couple these symmetries.

Thirdly, what does it mean that the order of applying the VEV matters? It is not necessarily unexpected that breaking a symmetry using different steps, leads to different (intermediate) symmetries. Different VEVs lead to different symmetry-breaking chains, so applying the VEVs in different orders does that too. However, how do we know what path nature takes? It should be investigated which order of VEVs is truly realised in nature and based on what characteristics of

the potential. To answer this, one would have to study the whole scalar potential and all relevant parameters. The work by Magnus Petz will be a great help in studying all this, but needs to be extended to all VEVs and symmetry-breaking paths that are possible. Only then can we see the whole picture and see what path nature takes, so either the **6** first, or the **10** VEV first. So, future physicists working on this area should address what conditions on the scalar potential enforce a particular VEV ordering and whether these different orderings can be distinguished phenomenologically, through their predictions for particle masses, or mixing angles, or proton decay rates. While both VEV orderings in this research reach the same residual symmetry A_4 , the intermediate symmetry structure differs, which can leave observable affects on the effective theory at lower energies.

Lastly, future researches might need to look into alternative discrete groups. In this research, we only looked into A_4 as a subgroup of $SU(3)$. As experiments improve, our A_4 -model might be ruled out. Other subgroups as S_4 or Δ_{27} might prove to give mixing angles closer to what we observe. The method on how to break $SU(3)$ presented in this research can be applied to these other subgroups as well.

5.3 Broader Implications

Besides the open questions, the research done here has quite some (possible) implications for physics.

5.3.1 Phenomenological implications of VEV ordering

The order-dependence we discovered in the breaking of $SU(3) \rightarrow A_4$ has implications beyond just mathematical curiosity. Different intermediate symmetries lead to different effective operators at intermediate energy scales. For the path with $SO(3)$ as intermediate symmetry versus $U(1) \times U(1) \times \Delta(3n^2)$, different generators are broken at different stages, which affects which operators appear in the effective theory below the GUT scale.

Consider for example proton decay predictions. The operators that mediate proton decay depend on which intermediate symmetry is preserved. If nature follows the **6**- VEV first, through $SO(3)$, certain decay chains are suppressed by the residual $SO(3)$ symmetry until the second breaking. The same for the **10**-first path through $U(1) \times U(1)$. Again different breaking chains dominate. This directly impacts our predictions for proton lifetime and branching rules.

5.3.2 Implications for Model Building

The findings in this thesis also demands that GUT model builders must specify both which scalar representation acquire VEVs and their hierarchy. Which VEV develops first is not arbitrary, but is determined by the structure of the scalar potential. The minimum of this potential dictates the VEV ordering and this in turn fixes the breaking chain and intermediate symmetries.

This adds a constraint to the construction of GUT models, that is often overlooked. Many researchers present their VEV textures without addressing their order, implicitly assuming that this does not matter. We have shown that this assumption is incorrect for the breaking of $SU(3)$ to A_4 . The same logic must be applied to other breaking paths. Whenever multiple VEVs are used, their

hierarchy must be justified by the potential structure, not chosen by preference or convenience.

So, while this research still gives us many open questions, we have taken a step forward in this research-chain, following Wouter Dekens [15], Jelle Thole [35] and Magnus Petz [32] in figuring out whether $SO(10)$ is indeed nature's perfect GUT and whether A_4 indeed governs flavour. The framework developed here helps future researchers to construct realistic models, test different breaking paths, and ultimately expose the symmetry principles that form the basis for particle physics.

Acknowledgements

I would like to first thank my supervisor Prof. Dr. Daniël Boer, for all his guidance, detailed feedback and for making the time to meet me every week. His patience in explaining the subtle points of group theory and his thorough comments on every draft were invaluable for this work.

I am grateful to Magnus Petz and Wouter Dekens, whose work on $SO(10)$ symmetry breaking and A_4 flavour symmetry laid essential groundwork for this research. They might not know it, but they have helped me a lot.

Besides my colleagues, I am also forever thankful for my dear friend Josephine van Driel, for proofreading my work and supporting me mentally. Then lastly I would like to thank my family, who despite their personal troubles, still supported me and cheered me on, every step of the way.

Bibliography

- [1] Guido Altarelli and Ferruccio Feruglio. “Tri-bimaximal neutrino mixing from discrete symmetry in extra dimensions”. In: 720 (Aug. 2005), pp. 64–88. DOI: 10.1016/j.nuclphysb.2005.05.005. (Visited on 07/24/2023).
- [2] Guido Altarelli and Ferruccio Feruglio. “Tri-bimaximal neutrino mixing, and the modular symmetry”. In: *Nuclear Physics B* 741 (May 2006), pp. 215–235. DOI: 10.1016/j.nuclphysb.2006.02.015.
- [3] F. P An et al. “Precision Measurement of Reactor Antineutrino Oscillation at Kilometer-Scale Baselines by Daya Bay”. In: *Physical Review Letters* 130 (Apr. 2022). DOI: 10.1103/physrevlett.130.161802.
- [4] Anthropic. *Claude*. 2025. URL: <https://claude.ai>.
- [5] M A Armstrong. *Groups and Symmetry*. Springer, 1988.
- [6] Michael Artin. *Algebra*. Pearson, 2017.
- [7] K. S. Babu and Ernest Ma. “Symmetry breaking in $SO(10)$: Higgs-boson structure”. In: *Physical Review D* 31 (May 1985), pp. 2316–2322. DOI: 10.1103/physrevd.31.2316. URL: <https://lib-extopc.kek.jp/preprints/PDF/1984/8412/8412241.pdf>.
- [8] K. S. Babu and R. N. Mohapatra. “Mass Matrix Textures from Superstring Inspired $SO(10)$ Models”. In: *Physical Review Letters* 74 (Mar. 1995), pp. 2418–2421. DOI: 10.1103/physrevlett.74.2418.
- [9] Stefano Bertolini, Luca Di Luzio, and Michal Malinský. “On the vacuum of the minimal nonsupersymmetric $SO(10)$ unification”. In: *Physical Review D* 81 (Feb. 2010). DOI: 10.1103/physrevd.81.035015.
- [10] Stefano Bertolini, Luca Di Luzio, and Michal Malinský. “The quantum vacuum of the minimal $SO(10)$ GUT”. In: *Journal of Physics: Conference Series* 259 (Nov. 2010), p. 012098. DOI: 10.1088/1742-6596/259/1/012098.
- [11] Daniël Boer. “Lie Groups in Physics”. In: (2022-2023).
- [12] Hong Thien An Bui. *Classifying the Finite Subgroups of $SO(3)$* . University of Chicago REU. 2020.
- [13] Nidal Chamoun et al. “Non-universal gaugino masses in supersymmetric $SO(10)$ ”. In: *Nuclear Physics B* 624 (Mar. 2002), pp. 81–94. DOI: 10.1016/s0550-3213(01)00652-6.
- [14] H. S. M. Coxeter. *Regular Polytopes*. 3rd. Dover, 1973.

[15] Wouter Dekens. *A4 family symmetry*. 2011. URL: https://fse.studenttheses.ub.rug.nl/9755/1/A4_family_symmetry.pdf.

[16] E. B. Dynkin. “Semisimple Subalgebras of Semisimple Lie Algebras”. In: *Transactions of the American Mathematical Society* (1952).

[17] Robert Feger and Thomas W Kephart. “LieART—A Mathematica application for Lie algebras and representation theory”. In: *Computer Physics Communications* (July 2014). DOI: 10.1016/j.cpc.2014.12.023.

[18] Robert Feger, Thomas W. Kephart, and Robert J. Saskowski. “LieART 2.0 – A Mathematica application for Lie Algebras and Representation Theory”. In: *Computer Physics Communications* 257 (Aug. 2020). DOI: 10.1016/j.cpc.2020.107490.

[19] R.M. Fonseca. “GroupMath: A Mathematica package for group theory calculations”. In: *Computer Physics Communications* (2021). DOI: 10.1016/j.cpc.2021.108085.

[20] Harald Fritzsch and Peter Minkowski. “Unified interactions of leptons and hadrons”. In: *Annals of Physics* 93 (Sept. 1975), pp. 193–266. DOI: 10.1016/0003-4916(75)90211-0.

[21] H. Georgi and S.L. Glashow. “Unity of All Elementary-Particle Forces”. In: *Physical Review Letters* 32 (Feb. 1974), pp. 438–441. DOI: 10.1103/physrevlett.32.438.

[22] W Grimus and P O Ludl. “Principal series of finite subgroups of $U(3)$ ”. In: *Journal of Physics A Mathematical and Theoretical* 43 (Oct. 2010). DOI: 10.1088/1751-8113/43/44/445209.

[23] A. Held, J. Kapisz, and L Sartore. “Grand unification and the Planck scale: an $SO(10)$ example of radiative symmetry breaking”. In: *Journal of High Energy Physics* (2022). DOI: 10.1007/jhep08(2022)122.

[24] Hugh F Jones. *Groups, Representations and Physics*. Institute Of Physics Publishing, 1998.

[25] Anjan S Joshipura and Ketan M Patel. “Fermion Masses in $SO(10)$ Models”. In: *Physical review. D. Particles, fields, gravitation, and cosmology/Physical review. D, Particles, fields, gravitation, and cosmology* 83 (May 2011). DOI: 10.1103/physrevd.83.095002.

[26] Christoph Luhn. “Spontaneous breaking of $SU(3)$ to finite family symmetries — a pedestrian’s approach”. In: *Journal of High Energy Physics* 2011 (Jan. 2011). DOI: 10.1007/jhep03(2011)108.

[27] Christoph Luhn and Pierre Ramond. “Anomaly conditions for non-Abelian finite family symmetries”. In: *Journal of High Energy Physics* 2008 (July 2008). DOI: 10.1088/1126-6708/2008/07/085.

[28] Ernest Ma and G. Rajasekaran. “Cobimaximal neutrino mixing from A_4 and its possible deviation”. In: *EPL (Europhysics Letters)* 119 (Aug. 2017), p. 31001. DOI: 10.1209/0295-5075/119/31001.

[29] S. Navas et al. “Review of Particle Physics”. In: *Phys. Rev. D* 110 (3 Aug. 2024), p. 030001. DOI: 10.1103/PhysRevD.110.030001. URL: <https://link.aps.org/doi/10.1103/PhysRevD.110.030001>.

- [30] OpenAI. *ChatGPT*. 2025. URL: <https://chat.openai.com/chat>.
- [31] Michael Edward Peskin and Daniel V Schroeder. *An Introduction to Quantum Field Theory*. Crc Press, 2019.
- [32] M. E. Petz. “SO(10) grand unification and its path to the Standard Model”. In: (July 2025). URL: <https://fse.studenttheses.ub.rug.nl/36170/1/mPHYS2025PetzME.pdf>.
- [33] Victoria Puyam, S Robertson Singh, and N Nimai Singh. “Deviation from Tribimaximal mixing using A4 flavour model with five extra scalars”. In: *Nuclear Physics B* 983 (Aug. 2022), pp. 115932–115932. DOI: [10.1016/j.nuclphysb.2022.115932](https://doi.org/10.1016/j.nuclphysb.2022.115932).
- [34] R. Slansky. “Group theory for unified model building”. In: *Physics Reports* 79 (Dec. 1981), pp. 1–128. DOI: [10.1016/0370-1573\(81\)90092-2](https://doi.org/10.1016/0370-1573(81)90092-2).
- [35] Jelle Thole. *Family symmetry Grand Unified Theories*. 2019. URL: <https://fse.studenttheses.ub.rug.nl/19026/1/ThesisFinalJelleThole.pdf>.
- [36] Anno Touwen. “Extending Symmetries of the Standard Model towards Grand Unification”. In: (2018).
- [37] Wolfram Research, Inc. *Mathematica 8.0*. Version 0.8. 2010. URL: <https://www.wolfram.com>.
- [38] Naoki Yamatsu. “Finite-Dimensional Lie Algebras and Their Representations for Unified Model Building”. In: *arXiv (Cornell University)* (2020). DOI: <https://doi.org/10.48550/arXiv.1511.08771>.
- [39] Masaki Yasuè. “Symmetry breaking of SO(10) and constraints on the Higgs potential”. In: *Physical Review D* 24 (Aug. 1981), pp. 1005–1013. DOI: [10.1103/physrevd.24.1005](https://doi.org/10.1103/physrevd.24.1005).
- [40] Jean-Bernard Zuber. *Generalized Dynkin diagrams and root systems and their folding*. 1997. URL: <http://arxiv.org/abs/hep-th/9707046v1>.

Chapter 6

Appendix

6.1 Generators of finite groups of $SU(3)$

The group generators of the finite subgroups of $SU(3)$ from [22] are listed here, with the following definitions:

$$\omega = e^{2\pi i/3}, \quad \epsilon = e^{4\pi i/9}, \quad \beta = e^{2\pi i/7}, \quad \mu_1 = \frac{1}{2}(-1 + \sqrt{5}), \quad \mu_2 = \frac{1}{2}(-1 - \sqrt{5}).$$

$$A(k) = \begin{pmatrix} 1 & 0 & 0 \\ 0 & e^{2\pi i/k} & 0 \\ 0 & 0 & e^{-2\pi i/k} \end{pmatrix}, \quad k = 1, 2, 3, \dots \quad (6.1a)$$

$$B = \begin{pmatrix} 0 & 0 & -1 \\ 0 & -1 & 0 \\ -1 & 0 & 0 \end{pmatrix} \quad (6.1b)$$

$$D = \begin{pmatrix} \epsilon & 0 & 0 \\ 0 & \epsilon & 0 \\ 0 & 0 & \epsilon \omega \end{pmatrix} \quad (6.1c)$$

$$E = \begin{pmatrix} 0 & 1 & 0 \\ 0 & 0 & 1 \\ 1 & 0 & 0 \end{pmatrix} \quad (6.1d)$$

$$F = \begin{pmatrix} -1 & 0 & 0 \\ 0 & 0 & -\omega \\ 0 & -\omega^2 & 0 \end{pmatrix} \quad (6.1e)$$

$$V = \frac{i}{\sqrt{3}} \begin{pmatrix} 1 & 1 & 1 \\ 1 & \omega & \omega^2 \\ 1 & \omega^2 & \omega \end{pmatrix} \quad (6.1f)$$

$$W = \frac{1}{2} \begin{pmatrix} -1 & \mu_2 & \mu_1 \\ \mu_2 & \mu_1 & -1 \\ \mu_1 & -1 & \mu_2 \end{pmatrix} \quad (6.1g)$$

$$X = \frac{1}{\sqrt{3}i} \begin{pmatrix} 1 & 1 & \omega^2 \\ 1 & \omega & \omega \\ \omega & 1 & \omega \end{pmatrix} \quad (6.1h)$$

$$Y = \begin{pmatrix} \beta & 0 & 0 \\ 0 & \beta^2 & 0 \\ 0 & 0 & \beta^4 \end{pmatrix} \quad (6.1i)$$

$$Z = \frac{i}{\sqrt{7}} \begin{pmatrix} \beta^4 - \beta^3 & \beta^2 - \beta^5 & \beta - \beta^6 \\ \beta^2 - \beta^5 & \beta - \beta^6 & \beta^4 - \beta^3 \\ \beta - \beta^6 & \beta^4 - \beta^3 & \beta^2 - \beta^5 \end{pmatrix} \quad (6.1j)$$

6.2 Generators of finite groups of $SO(3)$

The group generators of $SO(3)$ from [12], [5], [6], [14], are listed here. We use the following definition:

$$\phi = \frac{1}{2}(1 + \sqrt{5})$$

$$R = \begin{pmatrix} \cos(2\pi/k) & -\sin(2\pi/k) & 0 \\ \sin(2\pi/k) & \cos(2\pi/k) & 0 \\ 0 & 0 & 1 \end{pmatrix} \quad (6.2a)$$

$$x = \begin{pmatrix} 1 & 0 & 0 \\ 0 & \cos(2\pi/k) & -\sin(2\pi/k) \\ 0 & \sin(2\pi/k) & \cos(2\pi/k) \end{pmatrix} \quad (6.2b)$$

$$y = \begin{pmatrix} -1 & 0 & 0 \\ 0 & 1 & 0 \\ 0 & 0 & -1 \end{pmatrix} \quad (6.2c)$$

$$O_1 = \begin{pmatrix} -1 & 0 & 0 \\ 0 & -1 & 0 \\ 0 & 0 & 1 \end{pmatrix} \quad (6.2d)$$

$$O_2 = \begin{pmatrix} 0 & 0 & 1 \\ 1 & 0 & 0 \\ 0 & 1 & 0 \end{pmatrix} \quad (6.2e)$$

$$O_3 = \begin{pmatrix} -1 & 0 & 0 \\ 0 & -1 & 0 \\ 0 & 0 & -1 \end{pmatrix} \quad (6.2f)$$

$$I_1 = \begin{pmatrix} \frac{\phi-1}{2} & \frac{\phi}{2} & \frac{-1}{2} \\ \frac{-\phi}{2} & \frac{-1}{2} & \frac{1-\phi}{2} \\ \frac{-1}{2} & \frac{1-\phi}{2} & \frac{\phi}{2} \end{pmatrix} \quad (6.2g)$$

$$I_2 = \begin{pmatrix} \frac{1-\phi}{2} & \frac{\phi}{2} & \frac{1}{2} \\ \frac{-\phi}{2} & \frac{1}{2} & \frac{1-\phi}{2} \\ \frac{-1}{2} & \frac{\phi-1}{2} & \frac{\phi}{2} \end{pmatrix} \quad (6.2h)$$

$$I_3 = \begin{pmatrix} -1 & 0 & 0 \\ 0 & -1 & 0 \\ 0 & 0 & 1 \end{pmatrix} \quad (6.2i)$$

$$T_1 = \frac{1}{3} \begin{pmatrix} -1 & 2 & 2 \\ 2 & -1 & 2 \\ 2 & 2 & -1 \end{pmatrix} \quad (6.2j)$$

$$T_2 = \begin{pmatrix} 1 & 0 & 0 \\ 0 & -1 & 0 \\ 0 & 0 & -1 \end{pmatrix} \quad (6.2k)$$